MOLECULAR AND CELLULAR BIOLOGY, Oct. 2007, p. 7073–7088 Vol. 27, No. 20
0270-7306/07/$08.00+0 doi:10.1128/MCB.02116-06
Copyright © 2007, American Society for Microbiology. All Rights Reserved.

Drp1 Mediates Caspase-Independent Type III Cell Death in Normal and Leukemic Cells▽†

Marlène Bras,[1]‡ Victor J. Yuste,[1]‡ Gaël Roué,[1]‡ Sandrine Barbier,[1] Patricia Sancho,[1] Clémence Virely,[1] Manuel Rubio,[2] Sylvie Baudet,[3] Josep E. Esquerda,[4] Hélène Merle-Béral,[3] Marika Sarfati,[2] and Santos A. Susin[1]*

Apoptose et Système Immunitaire, CNRS-URA 1961, Institut Pasteur, 25 rue du Dr. Roux. 75015 Paris, France[1]; Centre de Recherche du CHUM, Hôpital Notre-Dame, Laboratoire d'Immunorégulation, 1560 Sherbrooke St. East, Montréal, QC H2L 4M1, Canada[2]; Service d'Hématologie Biologique, Groupe Hospitalier Pitie-Salpêtrière, Paris, France[3]; and Unitat de Neurobiologia Cellular, Departament de Ciencies Mediques Basiques, Facultat de Medicina, Lleida, Spain[4]

Received 13 November 2006/Returned for modification 14 February 2007/Accepted 24 July 2007

Ligation of CD47 triggers caspase-independent programmed cell death (PCD) in normal and leukemic cells. Here, we characterize the morphological and biochemical features of this type of death and show that it displays the hallmarks of type III PCD. A molecular and biochemical approach has led us to identify a key mediator of this type of death, dynamin-related protein 1 (Drp1). CD47 ligation induces Drp1 translocation from cytosol to mitochondria, a process controlled by chymotrypsin-like serine proteases. Once in mitochondria, Drp1 provokes an impairment of the mitochondrial electron transport chain, which results in dissipation of mitochondrial transmembrane potential, reactive oxygen species generation, and a drop in ATP levels. Surprisingly, neither the activation of the most representative proapoptotic members of the Bcl-2 family, such as Bax or Bak, nor the release of apoptogenic proteins AIF (apoptosis-inducing factor), cytochrome *c*, endonuclease G (EndoG), Omi/HtrA2, or Smac/DIABLO from mitochondria to cytosol is observed. Responsiveness of cells to CD47 ligation increases following Drp1 overexpression, while Drp1 downregulation confers resistance to CD47-mediated death. Importantly, in B-cell chronic lymphocytic leukemia cells, mRNA levels of Drp1 strongly correlate with death sensitivity. Thus, this previously unknown mechanism controlling caspase-independent type III PCD may provide the basis for novel therapeutic approaches to overcome apoptotic avoidance in malignant cells.

Programmed cell death (PCD) is a physiological "cell suicide" program essential for tissue homeostasis. Most organelles of the dying cell, including the endoplasmic reticulum (ER), Golgi apparatus, cytoskeleton, mitochondria, and lysosomes, undergo characteristic biochemical alterations, particularly partial proteolysis and permeabilization of membranes (18). In immune system regulation, the removal of cells was initially proposed to occur through a caspase-dependent apoptotic process. Although it seems clear that caspases are required for the typical apoptotic morphology, new data indicates that T- and B-cell elimination does not depend only on caspases (19, 52, 56, 71, 82). Alternative, caspase-independent models have therefore been proposed. Indeed, PCD can be divided into three different morphological and biochemical categories: type I, type II, and type III PCD (14, 28). Type I PCD consists of classical apoptotic cell death, characterized by cellular shrinkage, chromatin condensation, and DNA degradation. This apoptotic PCD is mediated by caspases and/or the mitochondrial apoptogenic protein cytochrome *c*, Omi/HtrA2, or Smac/DIABLO (35, 48). Type II PCD (or autophagic cell death) is characterized by the engulfment of cellular organelles such as mitochondria and ER by cytoplasmic vesicles, and it seems to involve the lysosomal cathepsins (28, 35). Type III PCD (also called necrosis-like PCD) is defined exclusively by cytoplasmic features (14, 35). The pathways incriminated in this last type of PCD are unfortunately poorly understood. In any case, type II PCD and type III PCD seem to operate in a caspase-independent manner (35).

CD47 (integrin-associated protein) is a widely expressed member of the immunoglobulin (Ig) superfamily, which functions both as a receptor for thrombospondin (TSP) and as a ligand for the transmembrane signal regulatory proteins SIRP-α and -γ. These molecules regulate various biological phenomena in the immune system, including platelet activation, leukocyte migration, and macrophage multinucleation (9). Importantly, they are involved in the negative regulation of the inflammatory response both in vitro and in vivo. For instance, CD47/TSP interaction negatively regulates antigen-presenting-cell and T-cell function in human cells (45). Moreover, TSP null mice display persistent inflammation in several organs (15), and CD47 null mice have impaired responses to bacterial pathogens (47) and defects in dendritic cell (DC) migration (30, 83). Most relevant to the present work, CD47 ligation, by TSP or immobilized CD47 monoclonal antibody (MAb), induces a form of caspase-independent cell death, which seems to be different from classical type I PCD (43, 44, 50, 53, 54, 58, 69).

Aberrant regulation of cell growth has traditionally been viewed as the major mechanism for tumor formation. However, it is clear that cellular changes leading to inhibition of apoptosis or PCD play an essential role in tumor development

* Corresponding author. Mailing address: Apoptose et Système Immunitaire, CNRS-URA 1961, Institut Pasteur, 25 rue du Dr. Roux, 75015 Paris, France. Phone: 33 1 40 61 31 84. Fax: 33 1 40 61 31 86. E-mail: susin@pasteur.fr.

† Supplemental material for this article may be found at http://mcb.asm.org/.

‡ M.B., V.J.Y., and G.R. should be considered first authors.

▽ Published ahead of print on 6 August 2007.

(90). The elucidation of the apoptotic pathways is thus an important area of study that may provide insight into the causes of drug resistance and facilitate the development of novel anticancer therapies. B-cell chronic lymphocytic leukemia (CLL) is the most common hematological malignancy in Western countries. Characterized by a progressive expansion of apparently quiescent B cells, CLL generally follows an indolent course. Despite the development of new chemotherapeutic agents that utilize the caspase-dependent pathway to provoke apoptosis, CLL is not considered curable (42). Future goals in CLL research are the identification of new factors sustaining the life span of the malignant B cells and the subsequent development of therapeutic agents that interfere with these molecules to provoke cell death. For this reason, the study of the molecular basis of alternative PCD pathways can provide new means of improving the current therapeutic strategies employed in the treatment of CLL.

The aim of the present work is to investigate the morphological, biochemical, and molecular mechanisms characterizing CD47-mediated PCD in normal and leukemic cells. Our approach shows that CD47 ligation induces a caspase-independent type III PCD process characterized by chymotrypsin-like serine protease activation, striking mitochondrial inner membrane alterations, loss of mitochondrial transmembrane potential ($\Delta\Psi_m$), production of reactive oxygen species (ROS), and outer leaflet exposure of phosphatidylserine (PS) in the plasma membrane. Importantly, our results lead us to identify a key mediator of type III PCD, dynamin-related protein 1 (Drp1) (86).

The unraveling of the mechanisms regulating CD47-mediated caspase-independent type III PCD should facilitate the understanding of alternate cell death pathways that take part in the control of immune cell homeostasis. In addition, induction of CD47-mediated caspase-independent PCD in CLL cells may be the basis for the development of novel anticancer therapies.

MATERIALS AND METHODS

Patients, B-cell purification, and culture conditions. After authorized consent forms were obtained, peripheral blood was collected from 5 healthy volunteers and from 30 CLL patients diagnosed according to classical morphological and immunophenotypic criteria (11). Patient characteristics are summarized in Table S1 in the supplemental material. These include clinical Binet staging (6) and biological parameters capable of predicting clinical course: mutational status of the IgVH gene, two "surrogate" factors (CD38 and ZAP-70), and soluble CD23. The IgVH gene sequence was determined as previously reported (61). Flow cytometric analysis of ZAP-70 was performed with an unconjugated anti-ZAP70 antibody (clone 2F3.2; Upstate) (16). CD38 and soluble CD23 expression levels were quantified using standard protocols (49, 68). All CLL patients used in this study have similar levels of CD47-positive cells (>90%). The Pitie-Salpetriere Hospital Institutional Ethics Committee approved this study. Mononuclear cells were purified from blood samples using a standard Ficoll-Hypaque gradient, and B cells were positively selected by magnetic beads coupled to anti-CD19 MAb (Miltenyi Biotech). Jurkat cells (clone E6; ATCC) and purified B cells were cultured in complete medium (RPMI 1640 medium supplemented with 10% fetal calf serum, 2 mM L-glutamine, and 100 U/ml penicillin-streptomycin).

Cell death induction and inhibition. To induce CD47-mediated cell death, cells were cultured at different times with soluble TSP (20 μg/ml; Calbiochem) or on precoated plates with CD47 MAb (5 μg/ml; clone B6H12). Alternatively, cells were treated for 20 h with hydrocortisone (HC) (0.5 mM) or brefeldin A-cycloheximide (5 μg/ml and 10 μg/ml, respectively); for 16 h with etoposide (5 μM), thapsigargin (10 μM), hydroxychloroquine (10 μM), dexamethasone (DEX) (1 μM), or Taxol (5 μM); for 6 h with staurosporine (STP) (1 μM); or for 3 h with H_2O_2 (10 mM). For protease inhibition assays, Q-VD.OPh (QVD) (10 μM), z-VAD.fmk, z-DEVD.fmk, z-VDVAD.fmk, z-VEID.fmk, z-LEHD.fmk, or z-IETD.fmk (50 μM); tosylsulfonyl phenylalanyl chloromethyl ketone (TPCK) (1 to 20 μM); *N*α-*p*-tosyl-L-lysine chloromethyl ketone (TLCK) (20 μM); MG101 (50 μM); *N*-acetyl-Leu-Leu-methional (50 μM); z-FA.fmk (100 μM); leupeptin (100 μM); or the proteasome inhibitors MG132, lactacystin, and NLVS (4-hydroxy-5-iodo-3-nitrophenylacetyl-Leu-Leu-leucinal-vinyl sulfone) (50 μM) (Merck Biosciences) were added 30 min before induction of cell death. Intracellular chymotrypsin-like, trypsin-like, and cathepsin activities were measured using Suc-Leu-Leu-Val-Tyr–7-amino-4-methylcoumarin (AMC), Boc-Leu-Arg-Arg-AMC, and Z-Arg-Arg-AMC (100 μM) (Calbiochem), respectively. Actinomycin D was used at 10 μM, cycloheximide at 100 μM, and bafilomycin A at 500 nM.

Flow cytometry. We used 40 nM $DiOC_6(3)$ for $\Delta\Psi_m$ quantification, 2 μM hydroethidine (Invitrogen) for the measurement of ROS generation, 100 nM LysoTracker Red (Invitrogen) for the quantification of lysosomal stability, annexin V-allophycocyanin (APC) (BD Biosciences) for the assessment of PS exposure, and propidium iodide for cell viability analysis. Chymotrypsin-like serine protease cytofluorometric detection was performed with a SerPase kit from Imgenex. Determination of Bax and Bak activation was performed as described previously (5), with MAbs designed to recognize the active form of Bax (MAb 6A7; BD Biosciences) or Bak (MAb Ab-1, Calbiochem), respectively. Data analysis was carried out in a FACScalibur (BD Biosciences) on the total cell population (10,000 cells).

Determination of ATP content. Cells treated as indicated were lysed, and the total ATP content was assessed with a luciferin-luciferase kit from Sigma. Luminescence was measured in a Berthold LB96V MicroLumat Plus. The ATP content is expressed relative to cell protein in arbitrary units.

DNA electrophoresis. Oligonucleosomal DNA fragmentation was detected by agarose gel electrophoresis as described elsewhere (65).

Caspase activity. Cells treated as indicated were lysed in caspase assay buffer containing 40 mM HEPES-NaOH (pH 7.2), 300 mM NaCl, 20 mM dithiothreitol, 10 mM EDTA, 2% Nonidet P-40, 20% sucrose, and 100 μM of Ac-DEVD-AFC. Caspase activity was read in a Fluoroskan Ascent fluorimeter (Thermo Labsystems).

Quantitative real-time reverse transcription-PCR. Total RNA from control or CLL cells was extracted with Trizol reagent (Invitrogen) according to standard procedures. Samples were examined in an ABI Prism 7000 sequence detector system with TaqMan Assays-on-Demand Gene Expression Products (Applied Biosystems). Data were analyzed using the comparative threshold cycle method according to the manufacturer's protocol. The amount of mRNA measured in CLL cells was normalized according to an endogenous reference (human 18S rRNA housekeeping gene) and relative to a calibrator (B cells from control donors).

Cell transfection and RNA interference assays. Jurkat cells were stably transfected either with pcDNA3.1 control vector (Jk-Neo) or with human Bcl-2, human Bcl-X_L (Jk-Bcl-2 and Jk-Bcl-X_L; inserts provided by J.L. Fernández-Luna, University Hospital of Santander, Spain), human Bcl-2 targeted to the ER (Jk-Bcl-2-ER; insert supplied by C. W. Distelhorst, University Hospital of Cleveland), or human Mcl-1 (Jk-Mcl-1; cDNA provided by I. Marzo, University of Zaragoza, Spain). For transient overexpression, Jurkat cells were transfected in a Nucleofector system (program S-18, kit V; Amaxa) with human Drp-1 (Jk-Drp1) and human Drp1 mutated in the GTPase domain (Jk-Drp1K38A and Jk-Drp1K679A inserts supplied by A.M. Van der Bliek, David Geffen School of Medicine at UCLA, and C. Blackstone, NINDS-NIH). For downregulation assays, Jurkat cells were similarly transfected with small interfering RNA (siRNA) double-stranded oligonucleotides designed against human Bax (5′-GGTGCCG GAACTGATCAGA-3′), Bak (5′-CCGACGCTATGACTCAGAG-3′), Bim (5′-TTACCAAGCAGCCGAAGAC-3′), Drp1 (Drp1a, 5′-GGTGCCTGTAGGTG ATCAA-3′; Drp1b, 5′-TCCGTGATGAGTATGCTTT-3′ [41]; Drp1c, 5′-CAG TATCAGTCTCTTCTAA-3′) or hFis1 (hFis1a, 5′-GCGGACAAGGTACAAT GAT-3′; hFis1b, 5′-AGGCATCGTGCTGCTCGAG-3′ [76]). As a control, we used an irrelevant oligonucleotide (5′-GCGATAAGTCGTGTCTTAC-3′) or an siRNA oligonucleotide against lamin A (5′-CTGGACTTCCAGAAGAA CA-3′). At 24 h after transfection, live cells were selected in a standard Ficoll gradient before cell death induction.

Protein extractions and immunoblotting. Mitochondrial and cytosolic fractions were obtained with the help of a kit from Pierce. Cell fractions and whole protein extracts from B lymphocytes or Jurkat cells were lysed in 20 mM Tris-HCl (pH 7.4), 150 mM NaCl, 1% Triton X-100, and 1 mM EDTA. Protein content was determined with the Bio-Rad DC kit, and 15 to 80 μg of protein was loaded on a sodium dodecyl sulfate-polyacrylamide gel. After blotting, polyvinylidene difluoride filters were probed with anti-human caspase 9 (Cell Signaling), anti-activated caspase 3 (BD Biosciences), anti-Bcl-2 (BD Biosciences),

anti-BclX_L (BD Biosciences), anti-Mcl-1 (BD Biosciences), anti-Bax (BD Biosciences), anti-Bak (BD Biosciences), anti-Bim (BD Biosciences), anti-AIF, anti-cytochrome *c*, anti-Smac/DIABLO (ProScience), anti-EndoG or anti-Omi/HtrA2 (Alexis), anti-Cox IV (Invitrogen), anti-β-tubulin or anti-DRP1/DLP1 (BD Biosciences), or anti-hFis1 (Alexis) or with antibodies against the mitochondrial respiratory chain (MRC) complex I subunits p39 (clone 20C11; Invitrogen) and p30 (clone 3F9, Invitrogen). All were detected with anti-mouse or anti-rabbit IgG–horseradish peroxidase conjugated according to standard procedures.

Recombinant proteins. N-terminal His-tagged Drp1, Drp1K38A, Drp1K679A, and Drp1(1–335) human recombinant proteins were produced from a Novagen pET28b expression vector and purified from *Escherichia coli* strain BL21 on a nickel-nitrilotriacetic acid affinity matrix column. The retaining extract, which contains the desired recombinant protein, was further purified onto a gel filtration chromatographic column (Superdex 200; Amersham). The eluted protein (≥95% purity) was stored in 50 mM HEPES (pH 7.9), 100 mM NaCl, 1 mM dithiothreitol, and 10% glycerol until use. Bax recombinant protein was from Abnova.

Cell-free system with isolated mitochondria. Mitochondria were isolated as previously described (79). Assessment of $\Delta\Psi_m$ was carried out by incubating 100 μg of mitochondria with 500 nM of the indicated recombinant protein in 80 nM rhodamine 123 (Invitrogen) and scoring by flow cytometry. For the mitochondrial swelling assay, 100 μg of mitochondria was incubated with recombinant Drp1, Drp1K38A, or Drp1K679A proteins (500 nM) and the A_{520} was recorded in an Ultrospec 3300 spectrophotometer (Amersham). For detection of cytochrome *c* release, mitochondria were incubated for 30 min at room temperature (RT) with the different recombinant proteins and then mitochondria were removed by centrifugation and supernatants and pellets were analyzed by immunoblotting.

Native gel electrophoresis. In situ detection of MRC complex I activity by native polyacrylamide gel electrophoresis was done as described previously (37, 72). Briefly, purified mitochondria were incubated with each recombinant protein for 30 min at RT and then loaded onto a 5 to 15% native polyacrylamide gel. Immediately after electrophoresis, the gel was incubated in 0.1 M Tris-HCl (pH 7.4), 1 mM NADH, and 2 mM nitroblue tetrazolium. The reaction was stopped with water after appearance of the band.

Oxygen consumption assessment. Mitochondrial respiration was measured in isolated mitochondria and digitonin-permeabilized cells using a Clark oxygen electrode (Oxygraph; Hansatech) as described previously (64). Substrate-driven respiration rates were measured as described previously (21) and expressed as nmol of O_2/min/mg of proteins. Complex I substrates and inhibitor were added at the following final concentrations: 5 mM malate, 5 mM glutamate, and 2 μM rotenone.

Cell growth measurements. Cell growth was analyzed using a Quantos cell proliferation assay kit (Stratagene) according to the manufacturer's instructions.

Detection of ROS in isolated mitochondria. Measurement of ROS in purified mitochondria was carried out by incubating 100 μg of mitochondria with 500 nM of the indicated recombinant protein in buffer containing 100 μM of the luminol analog L-012 (Wako) (17). Chemiluminescence was counted in a Berthold LB96V MicroLumat Plus.

Immunofluorescence and imaging. Cells labeled with 5 μM CellTracker Green (Invitrogen) and 1 μM Hoechst 33342 were subjected to Hoffman modulation contrast (HMC) or fluorescent microscopic assessment. Images were visualized in a Nikon Eclipse TE-2000-U fluorescence microscope with a Plan Apo 60×/1.4 objective, acquired with a Nikon Digital DXM 1200 camera, and analyzed using the Nikon ACT-1 2.2 software. May Grünwald-Giemsa (MGG) staining solutions were from Ral. In immunofluorescence experiments, cells were fixed with 4% paraformaldehyde and stained for the detection of activated Bax (MAb 6A7; BD Biosciences); activated Bak (MAb Ab-1; Calbiochem); calnexin, KDEL, and Hsp60 (Stressgen), DRP1/DLP1 (BD Biosciences); and cytochrome *c*, Smac/DIABLO, Omi/HtrA2, AIF, and EndoG. All were mounted with Vectashield and detected by anti-mouse or anti-rabbit IgG conjugated with Alexa Fluor (Invitrogen) according to standard procedures. The quantification of different parameters by fluorescence microscopy was performed in blind testing by at least two investigators, on 100 cells for each data point, and was repeated at least four times in independent experiments. Images were visualized at RT in an Apotome-equipped Zeiss Axioplan (Axiovert 200 M; Zeiss) with an Apochromat 100×/1.4 objective, acquired with a charge-coupled device Roper Scientific Coolsnap HQ camera, and analyzed using the Axiovision 4.4 software. MGG and Bax activation images were visualized at RT in a Nikon Eclipse TE-2000-U fluorescence microscope as described above.

Electron microscopy. Cells were fixed with 2% glutaraldehyde in phosphate buffer (pH 7.4) for 2 h at RT, washed, and postfixed in 2% OsO_4 before being embedded in Durcupan. Analysis was performed with a transmission electron microscope (Carl Zeiss MicroImaging), on ultrathin sections stained with uranyl acetate and lead citrate.

Statistical analysis. The significance of differences between experimental data included in Fig. 4A and B was determined using the Student *t* test for unpaired observations.

Unless specified, all reagents used were from Sigma-Aldrich.

RESULTS

Morphological and biochemical features of CD47-mediated cell death. In order to identify CD47-mediated cell death as one of the three types of PCD, we examined the morphological alterations induced by CD47 ligation. We first showed that after CD47 triggering, B lymphocytes isolated from CLL patients became nonviable, as determined by the fluorochrome CellTracker, which generates a fluorescent product only in live cells (Fig. 1A). The loss of viability provoked by CD47 triggering was confirmed by a cell growth assessment in which cells were quantified over time. As illustrated in the titration experiments included in Fig. 1B, the number of cells detected at 24, 36, or 48 h after CD47 ligation was significantly lower than the number of cells recorded among control cells. Indeed, the viability results presented in Fig. 1A and B fully confirm previous reports showing that CD47 ligation induces an unidentified form of PCD in leukemic T and B cells (44, 50, 53, 54, 65). Strikingly, in contrast to the apoptosis induced by HC, CD47-mediated PCD was not marked by signs of nuclear condensation, as shown by HMC light microscopy, Hoechst DNA staining, and MGG labeling (Fig. 1A). This fact indicates that CD47 ligation does not induce the classical type I PCD.

We next performed a more detailed ultrastructural study to identify potential modifications in intracellular organelles. CLL cells exposed to CD47 MAb exhibited a sequential alteration in their morphology (Fig. 1C). In the first step, the Golgi apparatus dilated, the ER redistributed around the nucleus, and mitochondria swelled slightly and underwent morphological change (Fig. 1C, panels c and e). No sign of autophagy (e.g., presence of intracellular vacuoles) was detected. At a later stage, cells became round and exhibited signs of karyolysis (Fig. 1C, panels d and f). We further confirmed the ER perinuclear redistribution and the Golgi dilation by immunodetection of these organelles by the resident ER transmembrane protein calnexin and the integral Golgi protein KDEL, respectively (Fig. 1D). The alterations in cellular organelles and the absence of autophagic vacuoles, a major hallmark of type II autophagic PCD, therefore classify CD47-induced cell death as type III or necrosis-like PCD (14, 35, 73).

Next, we characterized the biochemical events of CD47-mediated type III PCD. A detailed kinetic analysis confirmed that TSP and CD47 MAb-treated primary B cells underwent PS exposure, cell viability loss, $\Delta\Psi_m$ disruption, ROS production, and lysosomal permeabilization (Fig. 1E). Of note, pretreatment of cells with agents that block lysosomal function, such as bafilomycin A, did not prevent the PS exposure/cell viability loss associated with CD47 MAb treatment (see Fig. S1 in the supplemental material). This fact strongly suggests that lysosomal permeabilization is a secondary event in this type of PCD. CD47-mediated PCD is a rapid and time-dependent process, with significant alterations observed as soon as 30 min after treatment and a maximum effect at 6 h (Fig. 1E). In contrast, classical HC-induced type I PCD is a slower process,

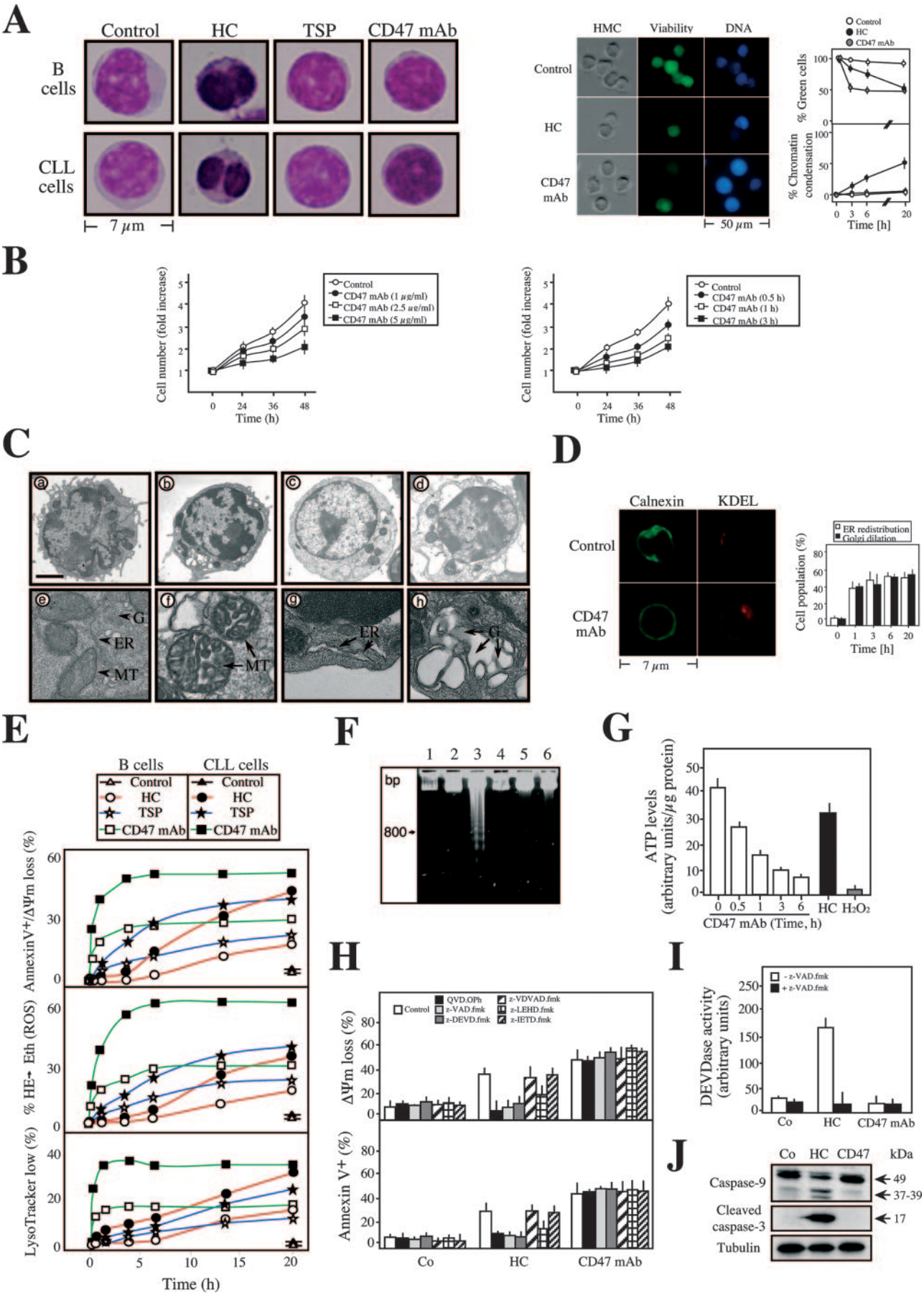
A
Control
HC
TSP
CD47 mAb
B cells
CLL cells
7 μm
HMC
Viability
DNA
Control
HC
CD47 mAb
50 μm
% Green cells
% Chromatin condensation
Time [h]
B
Cell number (fold increase)
Time (h)
CD47 mAb (1 μg/ml)
CD47 mAb (2.5 μg/ml)
CD47 mAb (5 μg/ml)
CD47 mAb (0.5 h)
CD47 mAb (1 h)
CD47 mAb (3 h)
C
G
ER
MT
D
Calnexin
KDEL
ER redistribution
Golgi dilation
Cell population (%)
E
B cells
CLL cells
AnnexinV+/ΔΨm loss (%)
% HE→ Eth (ROS)
LysoTracker low (%)
F
bp
800
G
ATP levels (arbitrary units/μg protein)
CD47 mAb (Time, h)
HC
H2O2
H
QVD.OPh
z-VAD.fmk
z-DEVD.fmk
z-VDVAD.fmk
z-LEHD.fmk
z-IETD.fmk
ΔΨm loss (%)
Annexin V+ (%)
I
- z-VAD.fmk
+ z-VAD.fmk
DEVDase activity (arbitrary units)
J
Co
HC
CD47
kDa
Caspase-9
Cleaved caspase-3
Tubulin
49
37-39
17

starting at 6 h and plateauing at 20 h. It is important to remark that CD47-mediated PCD does not require new transcription or translation. Indeed, CD47-mediated PCD is not modulated by actinomycin D or cycloheximide (see Fig. S2 in the supplemental material). Despite the aforementioned dysfunctions, CD47 MAb-treated cells did not show the biochemical hallmark of nuclear apoptosis, namely, oligonucleosomal DNA fragmentation, observed after HC treatment (Fig. 1F). Interestingly, the mitochondrial alterations observed after CD47 triggering (e.g., $\Delta\Psi_m$ loss and ROS generation) were coupled with a drop in cellular ATP levels (Fig. 1G). The cellular ATP pool diminished in a time-dependent manner with kinetics similar to those of CD47-mediated death, confirming that CD47 triggering provokes an effect on the levels of cellular ATP.

Next, we sought to determine the involvement of caspases in CD47-mediated PCD. First, we found that CD47-mediated PCD was not affected by the pan-caspase inhibitors QVD.OPh and z-VAD.fmk or by inhibitors of caspases 2, 3, 6, 7, 8, 9, and 10. As depicted in Fig. 1H, as opposed to the effect observed in the HC-mediated caspase-dependent PCD process, neither broad nor specific caspase inhibitors elicited a change in the mitochondrial damage or the PS exposure induced by CD47 ligation. Additional evidence that CD47 ligation does not induce caspase activity was seen using a fluorogenic substrate-based assay (Fig. 1I). This probe revealed a caspase 3/7 activity associated with HC-treatment and a residual activity, similar to that measured in control cells, in CD47 MAb-treated lymphocytes. Finally, we assessed the activation of two key players in caspase-dependent PCD: caspase 9 and caspase 3. These proteases are synthesized as inactive proenzymes of 49 and 32 kDa, respectively. After a caspase-dependent apoptotic insult, such as HC, caspases 9 and 3 are cleaved to yield active subunits of 37/39 and 17 kDa, respectively. Immunoblot analysis demonstrated that, in contrast to HC, caspase 9 or caspase 3 did not become activated even 6 h after CD47 MAb treatment (Fig. 1J). Overall, these results demonstrated that CD47-mediated PCD is a caspase-independent process.

Together, our results indicate that the cell damage induced by CD47 ligation is defined exclusively by cytoplasmic alterations. The morphological and biochemical features of CD47-mediated PCD represent the hallmarks of caspase-independent type III PCD.

The chymotrypsin-like family of serine proteases controls CD47-mediated killing. The absence of caspase activation led us to evaluate the possible effect of a specific family of proteases on the regulation of CD47-mediated cell death. Among the protease inhibitors tested, including inhibitors of trypsin-like proteases; calpains I and II; cathepsins B, D, and L; proteasome; and other general inhibitors of serine or cysteine proteases, only the chymotrypsin-like serine protease inhibitor TPCK maintained the cellular viability and mitochondrial function of CLL cells (Fig. 2A and B). As a control in this pharmacological approach, we verified that trypsin-like proteases, calpains, cathepsins, or proteasome inhibitors precluded other previously described types of PCD (1, 22, 23, 29).

FIG. 1. CD47 ligation induces caspase-independent type III PCD. (A) Normal cells (B cells) or CLL cells left untreated (control) or incubated with HC, TSP, or CD47 MAb for 1 h were stained with MGG to assess cellular morphology (left panels). Representative micrographs of each treatment are shown. Alternatively, B lymphocytes from a representative CLL donor were left untreated (control) or incubated with HC or CD47 MAb for 6 h before being stained with green fluorescent CellTracker and Hoechst 33342 to evaluate cellular viability and chromatin condensation. HMC microscopy was used to visualize cells (right panels). Representative micrographs of each stain are shown. The frequencies of green cells and nuclear chromatin condensation were determined by microscopic observation at the indicated times. Each point indicates the mean ± standard deviation from four independent experiments. (B) Growth rate assessment in CD47 MAb treated Jurkat T cells. Cells were cultured for 1 h in the presence of 1 to 5 μg/ml CD47 MAb, followed by quantification of cell number with a Quantos cell proliferation assay kit. Cells were seeded in 96-well plates, and the cell number was analyzed at the times indicated in a plate reader fluorometer. One unit refers to the fluorescence emitted by 25,000 cells. Values are means (± standard deviations) from four independent experiments (left panel). Representative results obtained from cells treated with 5 μg/ml CD47 MAb at different times are shown in the right panel. Cell numbers were quantified as described above. Data represent the means ± standard deviations ($n = 4$). CD47 ligation induces loss of viability, and consequently the number of cells measured after CD47 ligation was significantly lower than that for control cells. (C) Electron micrographs of CLL cells left untreated (panels a and e) or incubated with CD47 MAb for either 1 h (panels b and f to h), 6 h (panel c), or 16 h (panel d). Panel e demonstrates a typical example of the mitochondrial (MT), ER, and Golgi apparatus (G) normal morphology. Organelles are marked with arrowheads. Panels f, g, and h, respectively, show the mitochondrial morphology, ER dilation and redistribution, and Golgi swelling observed in CD47 MAb-treated cells. Organelles are marked with arrows. Bars: a to d, 1 μm; e to h, 100 nm. (D) In situ evidence of ER redistribution and Golgi apparatus dilation observed after CD47 MAb treatment. CLL cells were fixed and stained for immunodetection of the ER transmembrane protein calnexin and the *cis*-Golgi KDEL receptor. Representative micrographs are shown. The redistribution of each protein marker was quantified by microscopic observation at the indicated times. Each histogram indicates the mean ± standard deviation for three fields of at least 100 cells within a representative experiment. (E) Kinetic analysis of the PS exposure, cell viability, $\Delta\Psi_m$ dissipation, ROS production, and lysosomal permeabilization induced by TSP, HC, or CD47 MAb. After the indicated times, cells were labeled with $DiOC_6(3)$ and annexin V-APC, hydroethidine (HE), or LysoTracker Red. The data (means of a triplicate) obtained from a healthy donor or a representative CLL patient, after accounting for spontaneous apoptosis, are shown. This experiment was done four times, yielding low interexperiment variability (<5%). (F) Assessment of oligonucleosomal DNA fragmentation of CLL cells that were left untreated (lanes 1 and 2) or incubated with HC (lanes 3 and 4) or CD47 MAb (6 h) (lanes 5 and 6) in the absence (lanes 1, 3, and 5) or presence (lanes 2, 4, and 6) of the pan-caspase inhibitor z-VAD.fmk. (G) Quantification intracellular ATP levels in CLL cells treated at different times with CD47 MAb. HC and H_2O_2 were used as apoptotic and necrotic inducers, respectively. (H) Assessment of $\Delta\Psi_m$ loss and PS exposure in CLL cells preincubated with pan-caspase inhibitor QVD.OPh or z-VAD.fmk or with specific inhibitors of caspases 2 (z-VDVAD.fmk), 3 and 7 (z-DEVD.fmk), 9 (z-LEHD.fmk), or 8 and 10 (z-IETD.fmk) before induction of apoptosis by CD47 MAb (1 h) or HC. Results are the means ± standard deviations from five experiments. (I) Fluorometric measurement of caspase 3/7 activity observed in cytosolic extracts obtained from CLL cells untreated (Co) or treated with CD47 MAb (6 h) or HC in the absence or presence of the pan-caspase inhibitor z-VAD.fmk. Results are the means ± standard deviations from three experiments. (J) Total cell lysates from CLL untreated (Co) or treated with HC or CD47 MAb (6 h) were probed for the detection of activated caspase 9 or caspase 3. Arrows indicate the cleaved form of caspase 9 or 3, which is revealed only after HC treatment. Equal loading was confirmed by tubulin assessment.

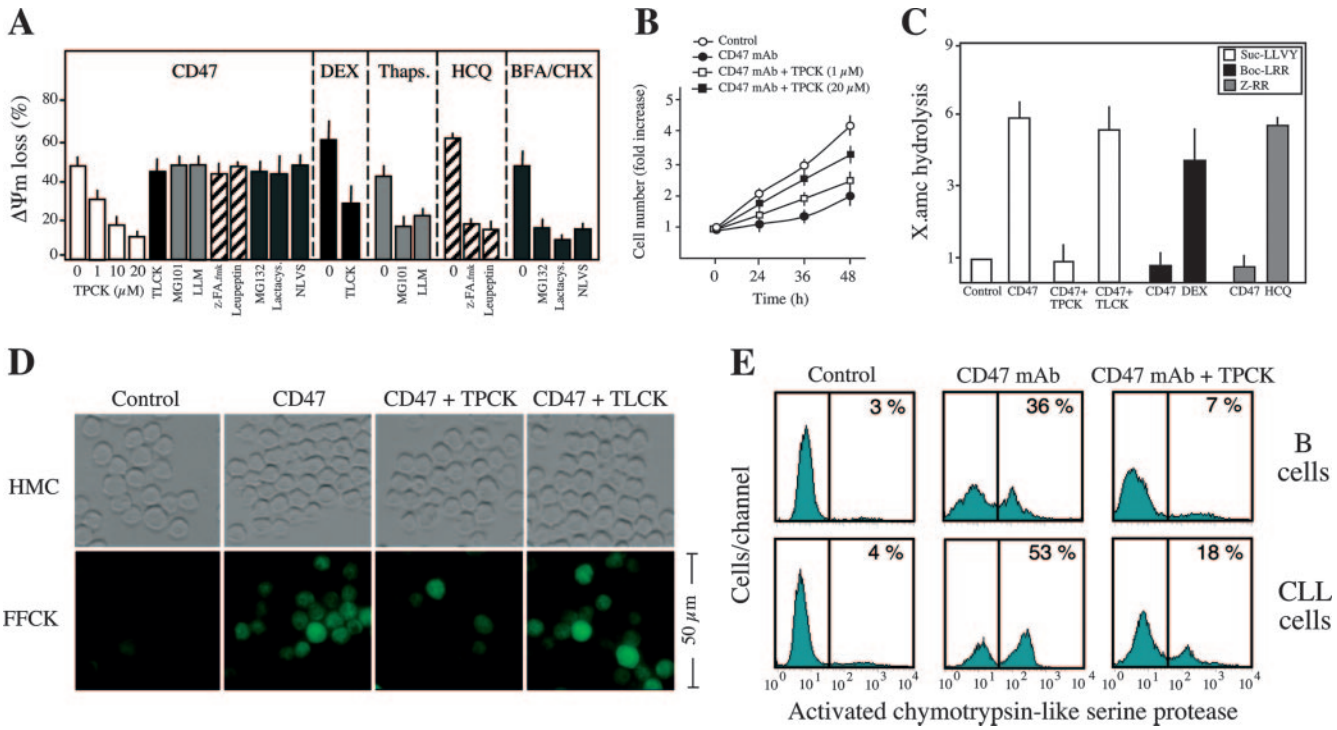

FIG. 2. Implication of chymotrypsin-like serine proteases in CD47-mediated cell death. (A) $\Delta\Psi_m$ loss induced by 1 h of CD47 ligation in CLL cells left untreated (time zero) or pretreated with inhibitors of chymotrypsin-like serine proteases (TPCK, at different concentrations), trypsin-like serine proteases (TLCK), type I or II calpains (MG101 and LLM), cathepsins B/D/L (z-FA.fmk and leupeptin), or proteasome (MG132, lactacystin, and NLVS). DEX, thapsigargin (Thaps.), hydroxychloroquine (HCQ), and brefeldin A/cycloheximide (BFA/CHX) were used as positive controls for trypsin-like, calpain, cathepsin, and proteasome activities, respectively. Data are means ± standard deviations from four independent experiments. (B) Effect of TPCK pretreatment on the inhibition of cell growth induced by CD47 ligation. Cells were cultured for 1 h in the absence (control) or presence of 5 μg/ml CD47 MAb, followed by quantification of cell number by a Quantos cell proliferation assay kit as for Fig. 1B. Alternatively, cells were pretreated with the inhibitor of chymotrypsin-like serine proteases TPCK at different concentrations before CD47 MAb treatment and proliferation was assessed as above. Note that TPCK reverses the effect of the CD47 MAb treatment. One unit refers to the fluorescence emitted by 25000 cells. Values are means (± standard deviations) from six independent experiments. (C) Fluorimetric measurement of chymotrypsin-like (Suc-AAPK.amc), trypsin-like (Boc-VLK.amc), and cathepsin (Z-RR.amc) protease activities observed in cytosolic extracts obtained from CLL cells incubated for 1 h with CD47 MAb in the absence or presence of the protease inhibitor TPCK or TLCK. One unit refers to the basal enzymatic activity measured in untreated cells. DEX and the lysosomotropic agent HCQ were used as positive controls for trypsin-like and cathepsin activities, respectively. Data are means ± standard deviations from four independent experiments. (D) B lymphocytes from CLL donors were left untreated (control), or incubated with CD47 MAb (1 h), CD47 MAb plus TPCK (20 μM), or CD47 MAb plus TLCK (20 μM) before assessment of chymotrypsin-like serine protease activity with a green fluorescent SerPase kit (FFCK). Representative micrographs of each treatment are shown. HMC microscopy was used to visualize cells. Note that TPCK significantly inhibits chymotrypsin-like serine protease labeling. (E) Normal B lymphocytes (B cells) or B lymphocytes from a CLL donor were left untreated (control) or incubated with CD47 MAb (1 h) or CD47 MAb plus TPCK (20 μM) before assessment of chymotrypsin-like serine protease activity as for panel D. Numbers indicate the percentage of cells positively stained. The experiment was repeated four times with a low variability (<5%).

Cytosolic extracts from CD47 MAb-treated cells, which contained a chymotrypsin-like TPCK-inhibitable protease activity but were devoid of either trypsin-like or cathepsin protease activity, supported our pharmacological conclusion (Fig. 2C). These results were further corroborated in normal and leukemic B cells by fluorescence microscopy (Fig. 2D) and flow cytometry (Fig. 2E) with the help of a fluorochrome-labeled TPCK analog that covalently binds to the active site of this subtype of serine proteases. In untreated cells, this analog yields negative results. However, after CD47 MAb ligation, B cells displayed a positive labeling, which is specifically inhibited by TPCK and not TLCK. Overall, these results demonstrate the involvement of chymotrypsin-like proteases in type III PCD. In addition, given that the inhibition of this type of protease suppresses the mitochondrial alterations characterizing CD47-mediated PCD (e.g., $\Delta\Psi_m$ loss), our data imply a hierarchical relationship between chymotrypsin-like serine proteases and mitochondria.

Mitochondrial alterations characterizing CD47-mediated PCD are independent of the most representative members of the Bcl-2 family of proteins. Mitochondria were morphologically and functionally altered in CD47-mediated PCD (Fig. 1), suggesting that the mitochondrion can act as a central coordinator of this kind of cell death. As reported previously, Bcl-2 proteins are regulators of the mitochondrial apoptotic pathway and can either suppress or promote mitochondrial changes (81). Bak, Bax, and Bim promote apoptotic cell death, whereas Bcl-2, Bcl-X_L, and Mcl-1 interfere with apoptotic activation (51). Thus, we assessed whether these Bcl-2 members could regulate CD47-mediated PCD. First, we quantified their mRNA expression by real-time PCR (Fig. 3A). Compared to B lymphocytes from healthy donors, CLL cells displayed a sig-

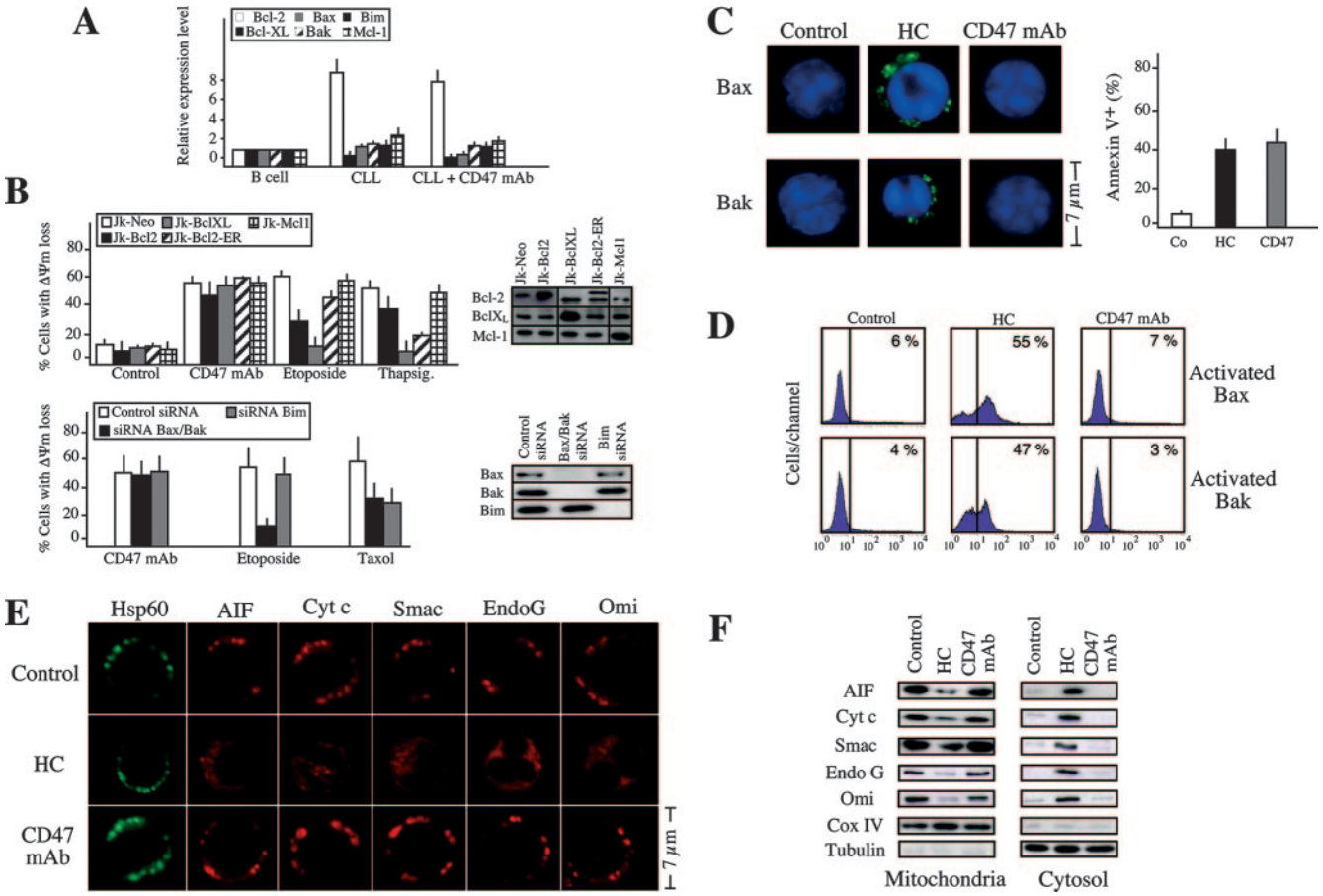

FIG. 3. CD47-mediated PCD functions independently of the most representative members of the Bcl-2 family of proteins. (A) Real-time reverse transcription-PCR quantification of Bcl-2, Bcl-X_L, Mcl-1, Bax, Bak, and Bim mRNA transcripts obtained from healthy B lymphocytes (B cell) ($n = 5$) or CLL B lymphocytes ($n = 15$) that were left untreated (CLL) or incubated 1 h with CD47 MAb (CLL + CD47). Results for CLL cells are expressed as the mean ± standard error of the mean. (B) Neither overexpression of Bcl-2, Bcl-X_L, or Mcl-1 nor downregulation of Bax, Bak, or Bim elicits a change in the mitochondrial damage induced by CD47 ligation. Jurkat cell lines were stably transfected with vector only (Jk-Neo) or cDNAs coding for human Bcl-2 (Jk-Bcl-2), human Bcl-XL (Jk-Bcl-XL), human Bcl-2 specifically targeted to the ER (Jk-Bcl-2-ER), or human Mcl-1 (Jk-Mcl-1). Bcl-2, Bcl-XL, and Mcl-1 expression levels were analyzed by Western blotting. After cells were treated with either CD47 MAb (1 h) or the inductor of apoptosis etoposide or thapsigargin, the frequency of cells with a low $\Delta\Psi_m$ was determined. Data are means ± standard deviations from four independent experiments. The effect of Bax, Bak, and Bim downregulation on the $\Delta\Psi_m$ loss provoked by the treatment of Jurkat cells with CD47 MAb (1 h), etoposide, or the microtubule-damaging agent paclitaxel (Taxol) is also shown. The frequency of $\Delta\Psi_m$ dissipation was assessed by $DiOC_6(3)$ labeling. Data are shown as mean values ± standard deviations for three independent experiments. Downregulation of Bax, Bak, or Bim was confirmed by Western blotting. (C) Immunofluorescent staining of activated Bax or activated Bak in CLL cells left untreated (control), or treated with HC or CD47 MAb for 1 h. Representative micrographs of each stain are shown. Enlargements are shown for detailing Bax or Bak activation. Note that only in HC-treated cells did Bax and Bax become stained (activated). As a control of cell death in this particular experiment, cells were stained with annexin V-APC and the frequency of positive labeling was recorded and illustrated as a plot. Data are means of a quadruplicate ± standard deviations. (D) Bax or Bak activation, quantified by flow cytometry, in CLL cells treated as for panel C. Numbers indicate the percentage of cells positively stained. The experiment was repeated three times with low variability (<5%). (E) CD47 ligation, unlike HC, does not induce release of apoptogenic proteins from mitochondria. Immunofluorescent detection of Hsp60 (used as a structural unreleased mitochondrial protein, green fluorescence), AIF, cytochrome *c* (Cyt c), Smac/DIABLO (Smac), EndoG, and Omi/HtrA2 (Omi) in CLL cells left untreated (control) or incubated with HC or CD47 MAb for 6 h is shown. Individual cells are representative of the dominant phenotype. This experiment was repeated eight times, yielding comparable results. (F) CLL cells were treated as for panel E. Mitochondrial and cytosolic extracts were analyzed by Western blotting for the presence of AIF, cytochrome *c* (Cyt c), Smac/DIABLO (Smac), EndoG, and Omi/HtrA2 (Omi). Cox IV and tubulin were used to control fractionation quality and protein loading.

nificantly higher level of Bcl-2 transcript. This fact suggests that CD47-mediated PCD proceeded even in the presence of elevated quantities of Bcl-2. Moreover, the ratio between the pro- and the antiapoptotic Bcl-2 members remained unchanged after CD47 ligation, indicating that this PCD operated independently of the transcriptional regulation of these Bcl-2 family members (Fig. 3A). In Jurkat T cells, we confirmed that none of these six Bcl-2 proteins controlled this form of PCD. In fact, neither overexpression of Bcl-2, Bcl-X_L, or Mcl-1 nor downregulation of Bax, Bak, or Bim elicited a change in the mitochondrial damage induced by CD47 ligation (Fig. 3B). However, overexpression of either Bcl-2 or Bcl-X_L or downregulation of Bax and Bak inhibited the $\Delta\Psi_m$ loss provoked by the PCD inductor etoposide (a topoisomerase II inhibitor) (Fig. 3B). When targeted to the ER, overexpressed Bcl-2 also prevented apoptosis induced by the ER calcium-

mobilizing agent thapsigargin (Fig. 3B), confirming previous work suggesting that Bcl-2 maintains Ca^{2+} homeostasis within the ER, thereby inhibiting apoptosis induction by thapsigargin (32). The death action of the microtubule-interfering reagent Taxol, which provokes the cytosolic-mitochondrial redistribution of the proapoptotic protein Bim (81), was significantly inhibited by the downregulation of this protein (Fig. 3B). Thus, our findings reveal that, in contrast to apoptosis caused by etoposide, thapsigargin, or Taxol, the mitochondrial dysfunctions characterizing CD47-mediated PCD are not controlled by the most representative members of the Bcl-2 family of proteins. An additional set of experiments validated these findings in CLL cells. In contrast to HC-treated cells, CD47 MAb-treated cells showed no activation of the proapoptotic proteins Bax and Bak (Fig. 3C and D). Moreover, this form of cell death proceeded without the release of the mitochondrial proapoptotic proteins AIF, cytochrome *c*, Smac/DIABLO, EndoG, and Omi/HtrA2 from mitochondria to cytosol (Fig. 3E and F).

Our results indicate that in CD47-mediated PCD, neither Bcl-2, Bcl-X_L, or Mcl-1 nor Bax, Bak, or Bim regulates $\Delta\Psi_m$ dissipation. Indeed, the lack of implication of these Bcl-2 family members could explain the absence of release of proapoptotic proteins from mitochondria in this mode of PCD.

Drp1 redistributes from cytosol to mitochondria after CD47 ligation. We next searched for a key element integrating the morphological and biochemical hallmarks of CD47-induced PCD. Accumulating evidence suggests that dynamin-related proteins, a family of proteins incriminated in mitochondrial remodeling (2, 10, 18, 46), establish a link between the mitochondrial dysfunctions cited above and PCD. Remodeling of mitochondria is controlled by the balance between fission and fusion and, more specifically, by the balance between Drp1 (33, 38, 74, 75, 86), Opa1 (13, 26, 34, 55), mitofusin 1 (Mfn1) (12, 67), and mitofusin 2 (Mfn2) (39). In this context, the striking mitochondrial inner membrane morphological changes observed in CD47-mediated PCD (Fig. 1C) led us to investigate the implication of these proteins in type III PCD. We thus quantified Drp1, Opa1, Mfn1, and Mfn2 mRNA expression in B cells from control donors and in B lymphocytes from 30 CLL patients described in Table S1 in the supplemental material. This analysis indicates that in most of the CLL patients tested, Drp1 and Mfn1, but not Opa1 or Mfn2, mRNA expression was high compared to that in B cells from control donors (Fig. 4A). Importantly, the Drp1 mRNA and protein expression strongly correlated with the susceptibility of B cells to CD47-induced PCD (Fig. 4A and B). Indeed, in patients 1 to 28 an elevated Drp1 expression level corresponds with a greater degree of responsiveness to CD47-mediated PCD, while patients 29 and 30, like subjects with normal B cells, presented both lower Drp1 expression and a poor cell death response to TSP and CD47 MAb (Fig. 4A and B; see Table S1 in the supplemental material). Interestingly, when comparing CD47-mediated PCD and HC-induced apoptosis in this panel of patients, CD47-mediated PCD represented a more efficient pathway to induce death. In fact, this comparative analysis distinguished three different types of response in CLL cells (Fig. 4B). In B cells from 19 patients (group 1), the response to TSP or CD47 MAb was comparable to that to HC treatment. CD47 ligation appeared to be a more efficient means of inducing PCD in B cells from nine patients (group 2), while in B cells from patients 29 and 30 (group 3) we observed a lower degree of death, similar to the level found in B lymphocytes from control donors. Overall, these results led us to further investigate the role of Drp1 in CD47-mediated PCD.

When redistributed from cytoplasm to mitochondria, Drp1 plays an essential role in the morphological changes observed during type I apoptosis (4, 7, 25, 40, 60, 66, 76). We showed that, after CD47 triggering, Drp1 translocated from cytoplasm to mitochondria in normal and leukemic cells in a time-dependent manner with kinetics similar to those for the CD47-mediated cell death response (Fig. 4C and D). Interestingly, we also showed that Drp1 redeployment strictly correlated with the response of CLL cells to CD47 triggering. In fact, mitochondrial relocalization of Drp1 was observed in a similar degree in B cells from CLL patients displaying a greater degree of responsiveness to CD47 ligation (e.g., patients 1 and 27) but to a lesser extent in B cells from a patient displaying poor cell death response to TSP or CD47 MAb (patient 30) (Fig. 4E). In contrast, Drp1 did not redistribute to mitochondria in HC-induced caspase-dependent apoptosis, suggesting that HC-mediated apoptosis utilizes a different molecular pathway than CD47-mediated PCD (Fig. 4E). These data strongly suggest that the localization of Drp1 in mitochondria is a central event in CD47-mediated PCD.

Drp1 induces mitochondrial damage and controls CD47-mediated PCD. Next, we established that Drp1 provokes the $\Delta\Psi_m$ collapse observed in CD47-induced PCD. After CD47 MAb triggering, cells transiently transfected with three different siRNAs designed against human Drp1 showed less pronounced $\Delta\Psi_m$ loss, as well as inhibition of PS exposure, than control siRNA-transfected cells (Fig. 5A). Thus, Drp1 gene silencing significantly attenuated CD47 MAb toxicity. This was further confirmed by a cell proliferation assay, which revealed that after CD47 MAb treatment, cell growth was significantly higher in Drp1-downregulated than in control transfected cells (Fig. 5B). This result indicates that Drp1-downregulated cells treated with CD47 MAb survived and, therefore, divided. Strikingly, in contrast to Drp1 gene silencing, overexpression of Drp1 sensitized cells to CD47 MAb (Fig. 5C). However, neither Drp1 downregulation nor Drp1 overexpression modulated apoptosis induced by HC, confirming that, as reported for other systems of type I PCD (57), this cell death pathway was Bax/Bak dependent (Fig. 3C) but Drp1 independent. Interestingly, two independent mutations in conserved lysines predicted to reduce the GTPase activity of Drp1 (K38 and K679) (75, 89) failed to inhibit CD47-mediated mitochondrial damage. Indeed, overexpressed Drp1K38A and Drp1K679A proteins, like Drp1, redistributed to mitochondria after CD47 triggering and sensitized cells to CD47-mediated PCD (Fig. 5C and D). These results indicate that the death function of Drp1 was independent of its GTPase activity in CD47-mediated PCD. In this way, pretreatment of cells with two compounds used to decrease intracellular GTP pools, mycophenolic acid and ribavirin, failed to inhibit CD47-mediated cell death (data not shown). Overall, our data indicate that Drp1 induced the $\Delta\Psi_m$ damage that characterized CD47-mediated type III PCD via a GTPase-independent mechanism.

In an attempt to establish a direct molecular link between the presence of Drp1 in mitochondria, $\Delta\Psi_m$ loss, and type III PCD, we tested whether downregulation of the mitochondrial

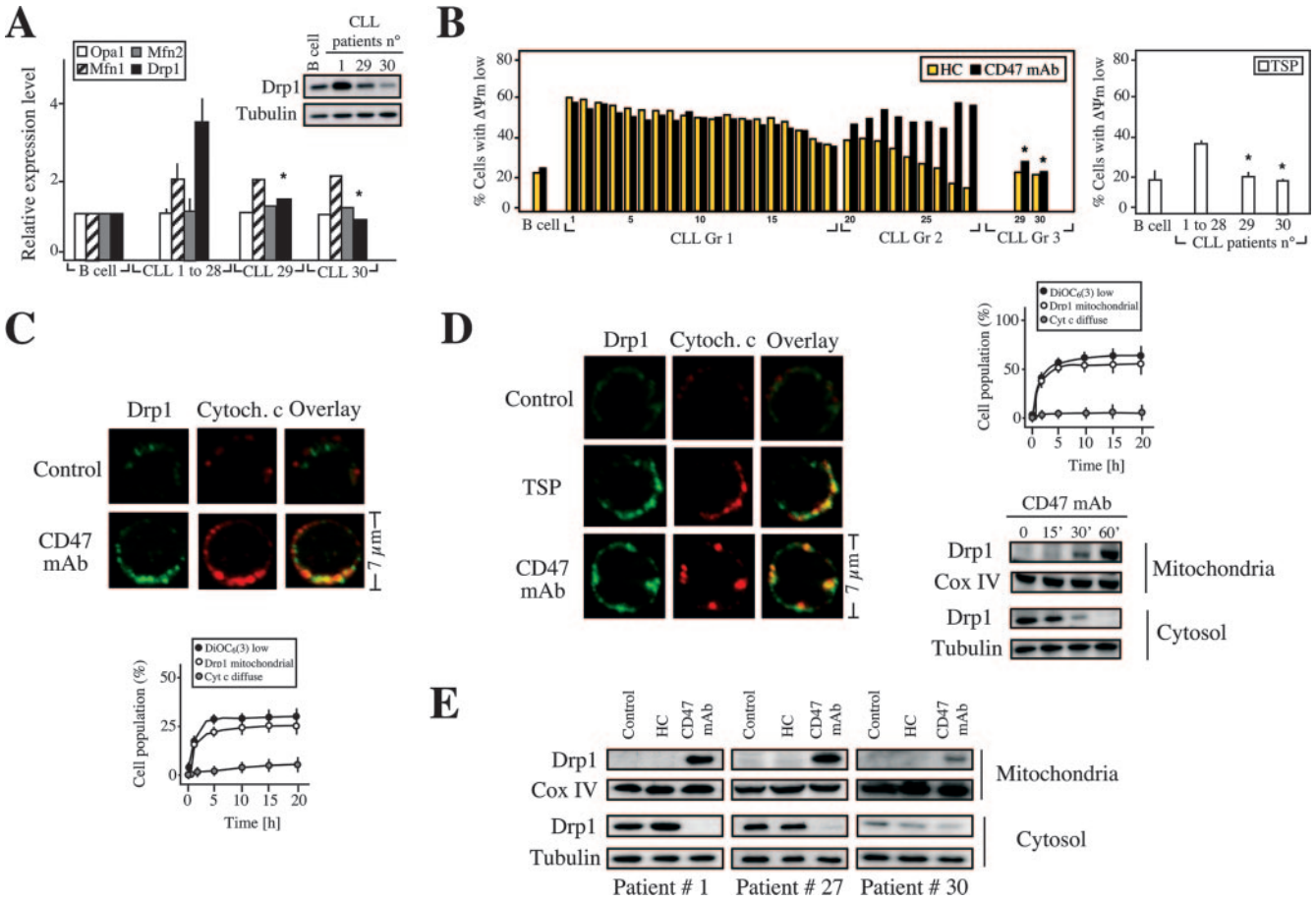

FIG. 4. Drp1 redistributes from cytosol to mitochondria in CD47-mediated PCD. (A) Real-time reverse transcription-PCR quantification of Opa1, mitofusin 1 (Mnf1), mitofusin 2 (Mnf2), and Drp1 mRNA transcripts purified from B lymphocytes from five control donors (B cell) or from 30 CLL patients (described in Table S1 in the supplemental material). Results for CLL patients 1 to 28 are expressed as the mean ± standard error of the mean. Total cell lysates from control B cells (B cell) along with B cells from three representative CLL patients (patients 1, 29, and 30) were prepared, and the Drp1 protein expression level was analyzed by Western blotting. Tubulin level was assessed in the same membrane as a loading control. Note that B lymphocytes from CLL patients 29 and 30, like normal B cells, showed lower Drp1 mRNA and protein expression. (B) B lymphocytes from a representative control donor (B cell) or B cells isolated from the 30 CLL patients used for panel A were cultured for 20 h in presence of CD47 MAb (black bars) or HC (yellow bars). The percentage of cells with $\Delta\Psi_m$ loss, after accounting for spontaneous apoptosis, is shown. Values are the means of a triplicate. Patients were divided into three groups according to their relative sensitivity to HC and CD47 MAb. In a similar set of experiments, B lymphocytes from control donors or CLL patients were treated with TSP and the percentage of cells with $\Delta\Psi_m$ loss was assessed. Results are expressed as the mean ± standard deviation ($n = 4$). *, $P < 0.001$ (unpaired Student t test). (C) Normal B lymphocytes were left untreated (control) or treated with CD47 MAb for 1 h and then stained for the detection of Drp1 and cytochrome *c* (Cytoch. c) (used as mitochondrial marker) before being examined by fluorescence microscopy. Representative cells show that Drp1 has a cytosolic distribution in control cells, whereas it colocalizes with cytochrome *c* in a mitochondrial staining pattern in CD47-treated cells. The numbers of cells showing low $\Delta\Psi_m$ (measured by flow cytometry), mitochondrial Drp1, or diffuse cytochrome *c* were quantified and plotted as a percentage of total cells. Data are the means ± standard deviations from five independent experiments. (D) CLL cells were left untreated (control) or treated with TSP (6 h) or CD47 MAb (1 h) and then stained for the detection of Drp1 or cytochrome *c*. The number of cells showing low $\Delta\Psi_m$, mitochondrial Drp1, or diffuse cytochrome *c* were quantified as for panel C. Kinetics of the Drp1 mitochondrial redeployment were detected by immunoblotting. After CD47 MAb treatment, CLL cells were subjected to subcellular fractionation, and mitochondrial and cytosolic fractions were blotted for Drp1 immunodetection. Fractionation quality and protein loading were verified by distribution of the specific subcellular markers Cox IV for mitochondria and tubulin for cytosol. (E) Immunoblot detection of Drp1 in mitochondrial and cytosolic fractions of control cells and cells stimulated with CD47 MAb for 1 h or treated with HC for 20 h. Cells were purified from a representative patient from each group identified in panel B. Cox IV and tubulin were used to control fractionation quality and protein loading. This experiment was repeated with cells purified from other patients from each group, yielding comparable results.

Drp1 binding protein hFis1 (36, 85, 87) regulated CD47-induced PCD. Transient transfection of two different siRNA double-stranded oligonucleotides designed against hFis1 alleviated the presence of Drp1 in mitochondria, along with $\Delta\Psi_m$ loss and PS exposure triggered by CD47 ligation (Fig. 5E). Thus, downregulation of Drp1 (Fig. 5A) or the mitochondrial Drp1 receptor hFis1 prevented CD47-mediated PCD, indicating that the presence of Drp1 in mitochondria is a key element in type III PCD.

We further generated the human Drp1 recombinant protein to investigate whether the mitochondrial alterations observed in CD47-mediated death were directly provoked by the protein

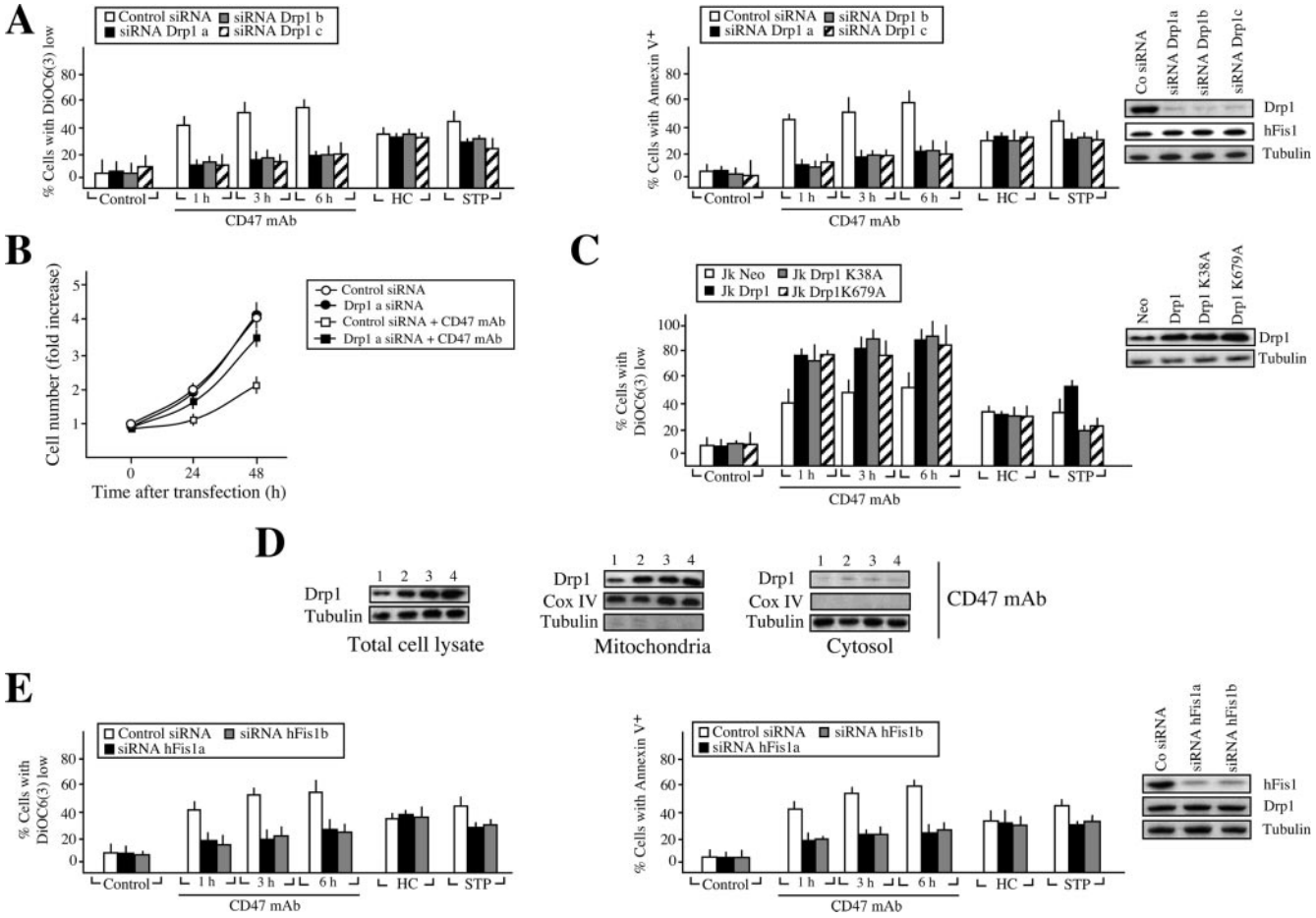

FIG. 5. Drp1 regulates CD47-mediated PCD. (A) Effect of Drp1 silencing on CD47-mediated death. Jurkat cells were transfected with a scramble or a lamin A siRNA double-stranded oligonucleotide (control siRNA) or with three different siRNA double-stranded oligonucleotides designed against human Drp1 (siRNA Drp1a, siRNA Drp1b, and siRNA Drp1c). Total cell lysates from control and Drp1 siRNA cells were prepared, and the expression level of Drp1 was analyzed by Western blotting. Analysis of hFis1 expression in these extracts confirms the specificity of Drp1 silencing. The tubulin level was also analyzed as a loading control. At 24 h after the indicated transfection, the $\Delta\Psi_m$ collapse or the PS exposure induced by treatment with CD47 MAb (1 to 6 h), HC, or the tyrosine kinase inhibitor STP was quantified by flow cytometry. Values are means ± standard deviations from five independent experiments. (B) Effect of Drp1 silencing on the CD47-mediated loss of viability. Jurkat cells were transfected with a control siRNA double-stranded oligonucleotide or with an siRNA double-stranded oligonucleotide designed against Drp1 as defined in panel A (Drp1a). At 24 h after the indicated transfection, cells were seeded in 96-well plates and the cell number was quantified as for Fig. 1B. Drp1 silencing, which precludes CD47-mediated cell death, contributes to cell growth. Data represent the means ± standard deviations ($n = 4$). (C) Drp1 overexpression promotes CD47-mediated $\Delta\Psi_m$ loss. Jurkat cells were transiently transfected with pcDNA3.1 vector only (Jk-Neo), human Drp1 cDNA (Jk-Drp1), and two cDNAs coding for human Drp1 mutated in its GTPase function, Drp1K38A (Jk-Drp1K38A) and Drp1K679A (Jk-Drp1K679A). The expression level of Drp1 was assessed by immunoblotting. Equal loading was controlled by tubulin detection. The $\Delta\Psi_m$ collapse induced by treatment with CD47 MAb (1 to 6 h), HC, or STP was quantified by flow cytometry as for panel A. Data represent the means ± standard deviations ($n = 6$). (D) Drp1, Drp1 K38A, and Drp1 K679A redistribute from cytosol to mitochondria after CD47 triggering. Jurkat cells were transiently transfected with pcDNA3.1 vector only (lanes 1), human Drp1 (lanes 2), human Drp1K38A (lanes 3), and human Drp1K679A (lanes 4) as for panel C. Total cell lysates were prepared, and the expression level of Drp1 was analyzed by Western blotting. The tubulin level was also analyzed as loading control. After treatment with CD47 MAb, cells were subjected to subcellular fractionation, and mitochondrial and cytosolic fractions were blotted for the immunodetection of Drp1. Fractionation quality and protein loading were verified by the distribution of the specific subcellular markers Cox IV for mitochondria and tubulin for cytosol. Immunodetection showed that, like Drp1, Drp1K38A and Drp1K679A redistribute from cytosol to mitochondria after CD47 ligation. (E) Effect of hFis1 silencing on CD47-mediated PCD. Jurkat cells were transfected with a control siRNA double-stranded oligonucleotide or with two siRNA double-stranded oligonucleotides designed against hFis1 (siRNA hFis1a and siRNA hFis1b). Immunodetection showed the changes in hFis1 expression. Analysis of Drp1 expression in these extracts confirms the specificity of hFis1 silencing. Equal loading was confirmed by tubulin detection. After CD47 MAb (1 to 6 h), HC or STP treatment, cells were stained with $DiOC_6(3)$ or annexin V-APC to quantify $\Delta\Psi_m$ dissipation or PS exposure, respectively. Data are shown as the means ± standard deviations ($n = 5$).

itself. In this way, Drp1, Drp1K38A, or Drp1K679A was exposed in a cell-free in vitro system to highly purified mitochondria. After incubation, mitochondrial features were monitored by four independent methods: cytofluorometry to measure $\Delta\Psi_m$, luminometry to assess ROS generation, spectrophotometry to quantify mitochondrial swelling, and immunoblotting to reveal cytochrome *c* release from mitochondria. Using these systems, we observed that the three recombinant proteins provoked $\Delta\Psi_m$ dissipation and ROS in isolated mitochondria in the absence of swelling or cytochrome *c* release (Fig. 6A, B, C,

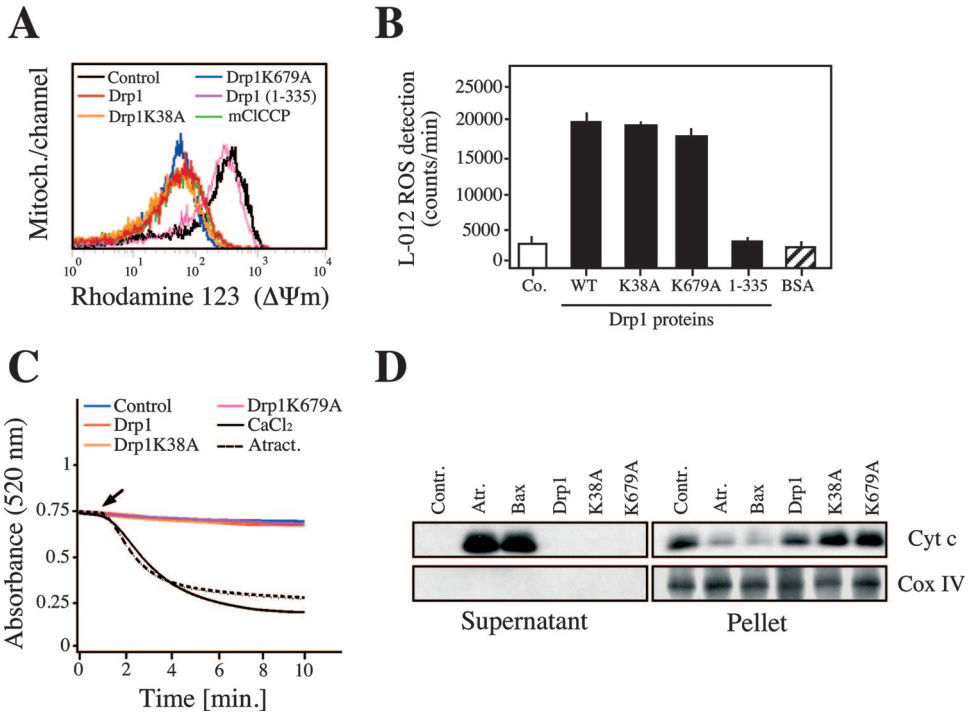

FIG. 6. Effect of Drp1, Drp1K38A, and Drp1K679A recombinant proteins on purified mitochondria. (A) Freshly isolated mitochondria were incubated with recombinant Drp1, Drp1K38A, or Drp1K679A protein, and the $\Delta\Psi_m$ was measured by flow cytometry as described in Materials and Methods. Each histogram represents the analysis of 50,000 events. The mitochondrial uncoupler mClCCP (1 μM) was used as a positive control, and the mutant protein Drp1(1–335) was used as a negative control. (B) Detection of ROS generated by Drp1, Drp1K38A, or Drp1K679A in mitochondria. Purified mitochondria (100 μg/ml) were diluted in buffer containing L-012 (100 μM), and ROS production was detected. Drp1(1–335) and bovine serum albumin (BSA) recombinant proteins were used as negative controls. Chemiluminescence was registered at intervals of 30 s over 5 min with a luminometer, and the signal was expressed as counts/min at 5 min. Data are means ± standard deviations from four independent experiments. (C) Experiments similar to those for panels A and B were performed to analyze mitochondrial swelling. A decrease in A_{520} is consistent with an increase in mitochondrial volume (31). As a control for mitochondrial swelling induction, atractyloside (5 mM) or $CaCl_2$ (100 μM) was used. Arrow, addition of each treatment. (D) Immunoblot of cytochrome *c* release detected in supernatants from mitochondria treated as for panel A, B, or C. Atractyloside (5 mM) and recombinant Bax (100 nM) were used as positive controls. Cox IV and pellet fractions were used to control fractionation quality and cytochrome *c* release.

and D). Indeed, Drp1, Drp1K38A, and Drp1K679A caused in vitro the same effects as those observed in TSP- or CD47MAb-treated cells. As a negative control in these experiments, we used an inactive Drp1(1–335) mutant protein, which failed to generate damage in purified mitochondria.

These results prove that Drp1 induced mitochondrial damage in a GTPase-independent manner, through a direct effect of the protein on mitochondria. But how did Drp1 induce mitochondrial dysfunction? Using two independent methods, (i) in situ detection of the electronic transport in MRC complex I (37, 72) and (ii) assessment of mitochondrial respiration in purified mitochondria, we confirmed that Drp1 impaired the electron transfer activity of the MRC (Fig. 7A and B). Therefore, the Drp1-mediated disruption of the MRC is likely to contribute to the $\Delta\Psi_m$ dissipation and the high ROS production observed during CD47-mediated PCD.

To extend these in vitro findings, we finally determined whether the MRC (e.g., complex I) was targeted during CD47-mediated PCD. CLL and Jurkat cells were treated at different times with CD47 MAb and permeabilized with digitonin, and mitochondrial respiration was assessed (Fig. 7C) (64). Like HC- or STP-treated cells, after CD47 ligation, CLL or Jurkat cells failed to respire (Fig. 7C). Strikingly, a reduction in the mitochondrial respiration rate was produced with kinetics similar to those of CD47-mediated $\Delta\Psi_m$ dissipation, ROS production, and ATP loss (Fig. 1E and G and 7C). These data strongly suggest that CD47 ligation provokes disruption of MRC through the massive relocalization of Drp1 in mitochondria. Accordingly, TPCK, a pharmacological agent that inhibits CD47-mediated type III PCD and blocks the relocalization of Drp1 in mitochondria (Fig. 2 and data not shown), restored the normal mitochondrial respiration rate in CD47 MAb-treated cells (Fig. 7C).

Together, these results showed that following CD47 ligation, Drp1 redistributes to mitochondria (Fig. 4C and D), where the protein provokes impairment of MRC activity (Fig. 7), loss of $\Delta\Psi_m$ (Fig. 1C and 6A), production of ROS (Fig. 1C and 6B), ATP loss, and disruption of the mitochondrial structure (Fig. 1C).

DISCUSSION

In this report, we have elucidated some of the mechanisms of the least-characterized mode of cell death, caspase-independent necrosis-like (or type III) PCD. Our data, obtained mainly from normal B cells and from B lymphocytes from

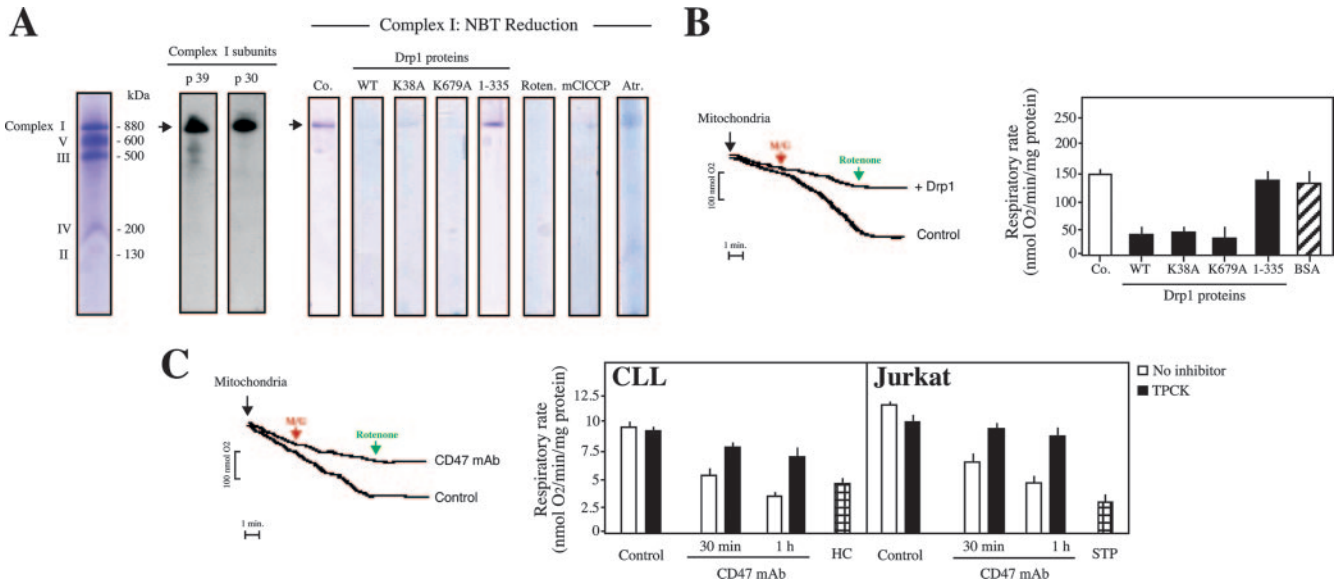

FIG. 7. Drp1 impairs mitochondrial electron transport. (A) Drp1, Drp1K38A, or Drp1K679A mitochondrial electron transfer inhibition measured by in situ MRC complex I activity detection. MRC complex I was visualized by Coomassie blue staining (left) or by specific Western blot detection. Treatment with rotenone (20 μM), a complex I inhibitor which blocks the reduction of nitroblue tetrazolium and prevents the detection of the complex I band, confirms the specificity of the reaction. Atractyloside and mClCCP were used as positive controls, and Drp1(1–335) was used as a negative control. (B) Drp1, Drp1K38A, or Drp1K679A blocks mitochondrial respiration in response to complex I substrates. Mitochondria (400 μg) were left untreated (control) or incubated with Drp1 (500 nM), and oxygen consumption was measured in a Clarke-type electrode. Representative curves are shown. Malate and glutamate (M/G) were added at 5 mM and rotenone at 2 μM. In a similar set of experiments, mitochondria were treated with Drp1, Drp1K38A, Drp1K679A, or the negative control Drp1(1–335) or bovine serum albumin (BSA) and analyzed for oxygen uptake. Rates of O_2 consumption were calculated and expressed as nmol of O_2/min/mg of protein. Data are means ± standard deviations from four independent experiments. (C) Oxygen consumption in CD47-treated cells. CLL or Jurkat cells were left untreated or pretreated with TPCK before being treated with CD47 MAb at different times. Alternatively, cells were incubated with HC or STP. Cells were then permeabilized with digitonin, and 400 μg of protein was loaded into the respiratory chamber. Oxygen consumption in presence of the complex I substrate M/G (5 mM each) was measured as for panel B. Representative curves obtained for untreated (control) cells or cells treated with CD47 MAb (1 h) are shown. Rates of O_2 consumption were calculated and expressed as nmol of O_2/min/mg of protein as for panel B. Data are means ± standard deviations from five independent experiments.

patients suffering from CLL, demonstrate that CD47-mediated PCD proceeds via the induction of atypically regulated mitochondrial alterations that are independent of some of the major apoptotic effectors, such as Bax or Bak, and caspases. Indeed, the results presented here are the first published report of massive mitochondrial alterations induced without the involvement of caspases, the Bcl-2 family of proteins, or the release of apoptogenic proteins from mitochondria. In characterizing Drp1 as a key element in caspase-independent type III PCD, we also provide insight into the molecular mechanisms governing this type of PCD. Briefly, we show that ligation of the CD47 receptor leads, by means of the chymotrypsin-like proteases, to translocation of Drp1 from cytosol to mitochondria, where the protein induces MRC damage, $\Delta\Psi_m$ dissipation, ROS generation, and ATP loss. These mitochondrial alterations (e.g., massive ROS production) may certainly enhance the damage to other organelles, such as the ER, lysosomes, and Golgi apparatus, facilitating the execution of this necrotic cell death pathway.

Nevertheless, type III CD47-mediated cell death shares common features with the other two forms of PCD. Certain biochemical features are conserved, namely, outer leaflet exposure of PS in the plasma membrane, alterations to mitochondria and lysosomes, and production of ROS. In addition, all three forms of PCD are marked by a dependence on input from several cellular compartments, the most important being the mitochondrion. In CD47-mediated type III PCD, four main observations support this last assertion. First, impairment of the MRC, a fall in the $\Delta\Psi_m$, and the concomitant ROS generation and ATP loss are constant features of this type of PCD. Second, from the available biochemical data, it appears that this kind of cell death does not require the participation of other proapoptotic organelles, such as lysosomes (e.g., through cathepsin B, D, or L activity). Third, inhibitors of the mitochondrial modifications induced by CD47 ligation (e.g., TPCK) abolish CD47-mediated PCD. Finally, downregulation of the Drp1 mitochondrial receptor hFis1 precludes the $\Delta\Psi_m$ loss and PS exposure which are associated with CD47 triggering. Together these data are compatible with the hypothesis that $\Delta\Psi_m$ disruption constitutes a key event in type III PCD. The direct cause-effect relationship between the mitochondrial and cytoplasmic manifestations of type III PCD further underlines the central role of mitochondria in the regulation of this type of cell death.

Control of the Drp1 redistribution mediated by the chymotrypsin-like serine proteases was essential to an understanding of the interplay between the multiple CD47-induced signals. Our results indicate that activity of the chymotrypsin-like family of serine proteases allows Drp1 redistribution from cytosol to mitochondria in CD47-mediated PCD. Thus, as in other types

of cell death (3, 84), Drp1 redistributes from cytosol to mitochondria in a specifically controlled manner. Further analysis is necessary to identify the serine protease involved in this kind of cell death. In any case, our results place the chymotrypsin-like family of serine proteases at an early premitochondrial step in caspase-independent type III PCD.

Normally residing in cytoplasm, Drp1 translocates under apoptotic conditions to mitochondria, where it interacts with its mitochondrial partner, hFis1 (36, 76, 85). This mitochondrial translocation is Ca^{2+} dependent in some types of apoptosis (8, 27). In apparent contradiction to the data reported here, it has been reported that Drp1 and Bax colocalize in mitochondria to induce mitochondrial fission and caspase-dependent cell death (39, 40). As in etoposide or nitric oxide PCD (4, 77), this kind of caspase-dependent PCD relates to the GTPase function of Drp1. In this context, the GTPase-inactive Drp1 mutant Drp1K38A blocks STP- or etoposide-induced mitochondrial fission, $\Delta\Psi_m$ loss, cytochrome *c* release, and type I apoptosis (39, 77). In HC-mediated caspase-dependent killing, our data indicated that Bax activation was not coupled to Drp1 translocation (Fig. 3C and D). Consequently, HC-mediated PCD is not regulated by overexpression or downregulation of Drp1. In the same way, a recent study confirms that in caspase-dependent PCD induced by actinomycin D or UV irradiation, downregulation of Drp1 or hFis1 does not inhibit Bax-dependent apoptosis (57). Finally, in caspase-independent CD47-mediated type III PCD, the mitochondrial alterations provoked by Drp1 translocation (e.g., $\Delta\Psi_m$ collapse and ROS generation) occur in the absence of Bax activation (Fig. 3C and D), release of mitochondrial apoptogenic proteins (Fig. 3E and F), or mitochondrial fission (J. E. Esquerda and S. A. Susin, unpublished observation). Thus, depending on the form of PCD, it seems that Bax and Drp1 could be coupled or uncoupled in the induction of mitochondrial alterations and cell death.

Interestingly, the mitochondrial dysfunctions monitored in CD47-mediated PCD are independent of the GTPase function of Drp1. In fact, overexpression of wild-type Drp1 or the GTPase-deficient Drp1 mutants Drp1K38A and Drp1 K679A provokes a similar degree of responsiveness to CD47-mediated PCD. This apparent paradox in Drp1 mitochondrial function may reflect the fact that Drp1 is likely to be a bifunctional protein in PCD with a fission, GTP-dependent function and an alternate mitochondrial cell death function. In this way, two recent reports have shown that Drp1 mitochondrial targeting is independent of the GTPase activity of the protein (59) and that Drp1 has other functions in mitochondria that differ from fission regulation (27). A third study has demonstrated that deletion of the hFis1 α1-helix inhibits mitochondrial fragmentation but strongly enhances interaction between Drp1 and hFis1. This interaction, which depends on the region from amino acid 61 to 91of hFis1, provokes the same features as those observed in CD47-mediated death: mitochondrial swelling in absence of cytochrome *c* release (87). These reports and our data strongly favor the hypothesis that massive and specific targeting of Drp1 to the mitochondrial surface and interaction with partners proteins such as hFis1 cause mitochondrial dysfunction. However, other proteins, such as Bax, are needed to induce the release of apoptogenic proteins from mitochondria or to facilitate mitochondrial fission. In STP- or etoposide-mediated PCD, caspase activity or Bax function may enhance Drp1 mitochondrial activity, causing both the release of pro-apoptotic proteins from mitochondria and the mitochondrial outer membrane modifications that, in cooperation with the GTPase-dependent mechanochemical properties of Drp1, lead to mitochondrial fission. In this context, the lack of implication of caspase and Bax in CD47-mediated PCD explains the absence of both mitochondrial fission and release of apoptogenic proteins.

Cell-free systems have been extremely valuable for the analysis of apoptosis mechanisms (24, 78). Using this in vitro system we demonstrated that, once in mitochondria, Drp1 induced a dramatic decrease in $\Delta\Psi_m$. Surprisingly, this mitochondrial alteration was not accompanied by mitochondrial swelling or cytochrome *c* release. In fact, we showed that Drp1 blocked the electron transport activity of MRC and provoked massive ROS generation. In this sense, it is known that electron transport impairment results in $\Delta\Psi_m$ loss, massive ROS production, and lack of ATP generation (31), and that is exactly the picture observed in CD47-mediated PCD. With kinetics similar to those of CD47-mediated Drp1 redistribution, $\Delta\Psi_m$ loss, ROS production, and ATP decrease, we confirmed the dysfunction of MRC in CLL and Jurkat cells subjected to CD47 ligands. Thus, as in caspase-dependent type I PCD (63, 64), the loss of MRC function was implicated in the mitochondrial damage characterizing caspase-independent type III PCD. A more detailed study should be developed to identify whether Drp1 provokes the dysfunction of the MRC electron transport directly, by action on a specific complex (e.g., complex I), or indirectly, by provoking a general MRC disorganization. If the "direct" action applies, important questions need to be resolved. How does the connection between Drp1 (on the outer mitochondrial membrane) and MRC (on the inner mitochondrial membrane) take place? Does Drp1 translocate from the outer to the inner mitochondrial membrane to disrupt mitochondrial electronic transport? Does Drp1 inhibit MRC complex II, III, or IV activity? In the second, "indirect" situation, it seems possible that the presence of Drp1 in mitochondria, which provokes a disorganization of the mitochondrial structure (Fig. 1C), enables a mechanical rupture of the mitochondrial inner membrane. This certainly impairs normal MRC electron transport activity. In our hands, this possibility applied in the pretreatment of purified mitochondria with atractyloside, a ligand of the mitochondrial adenine nucleotide transporter. Atractyloside induced mitochondrial swelling that, in turn, provoked a mechanical rupture of mitochondrial membranes (88). As a consequence, mitochondrial electronic transport was impaired (e.g., as depicted in Fig. 7A). Another example of "indirect" MRC impairment is the pretreatment of mitochondria with the uncoupler mClCCP (carbonyl cyanide *m*-chlorophenylhydrazone) which also blocks complex I activity (Fig. 7A). In any case, our data fully confirm that in CD47-mediated type III PCD, the action of Drp1 on mitochondria provokes impairment of MRC I activity (Fig. 7), loss of $\Delta\Psi_m$ (Fig. 1C and 6A), production of ROS (Fig. 1C and 6B), ATP loss, and disruption of the mitochondrial structure (Fig. 1C). Of course, it would be of great interest to study whether this novel Drp1 function in type III PCD can be extended to other cell types or PCD pathways (e.g., caspase-dependent type I PCD).

Our experiments, performed with B cells from control donors and a large number of CLL patients, showed that CD47 ligation provoked cell death rapidly, with a higher efficacy in CLL cells than in normal B cells, and more efficiently than HC-mediated apoptosis. Interestingly, sensitivity to CD47-mediated PCD strongly correlated with the expression of Drp1, making Drp1 a potential marker for PCD susceptibility. Our data demonstrate the existence of a biochemical caspase-independent pathway in primary malignant B cells that could be regulated independently of the caspase-dependent pathway. In fact, in CLL, accumulation of B cells reflects their resistance to "classical" caspase-dependent apoptosis. Hence, the study of the molecular basis of alternative cell death pathways can provide new means of improving the current therapeutic strategies employed in the treatment of this disease.

Together with the biochemical mechanisms proposed to mediate CD47-induced PCD in normal and leukemic T cells (43, 44, 50, 62, 69), our observations in primary B cells lead us to conclude that CD47 and its two ligands, TSP and SIRP-α, could participate in the elimination of cells during the immune response. In that sense, TSP, secreted by macrophages and DCs at a steady state and during an inflammatory process, may contribute to the maintenance of immune homeostasis. First, TSP/CD47 interaction serves as an autocrine negative regulator of DC maturation and function (20). Second, TSP/CD47 induces caspase-independent PCD in lymphoid cells, sparing the DCs, followed by the engulfment of the dying cells by professional phagocytes (53). Notably, the expression of CD47 on apoptotic cells is required to allow their in vitro phagocytosis by APC (80). Third, TSP establishes "a molecular bridge" between apoptotic cells and phagocytes, facilitating the clearance of dying cells (70).

In conclusion, our work reveals substantial progress in two major areas: (i) in the understanding of the molecular events regulating caspase-independent type III PCD in normal and leukemic cells and (ii) in the development of new approaches to CLL treatment. In fact, the identification of a "downstream" death effector of CD47-mediated PCD, such as Drp1, might pave the way for novel diagnostic and pharmacological strategies for the treatment of this malignancy.

ACKNOWLEDGMENTS

We thank M. Segade and S. Pellegrini for critical comments and C. Artus, C. Delettre, S. Beaucourt, B. Queenan, S. Laine, R. S. Moubarak, and N. Robert for invaluable help.

This work was supported by institutional grants from Institut Pasteur and CNRS and by specific grants from Fondation de France, Ligue Contre le Cancer, and Association pour la Recherche sur le Cancer (contract no. 4043) (to S.A.S.), as well as grants from the Spanish Ministry of Education and Science (grant 2005-01535) (to J.E.E.), the Canadian Institute for Health and Research (grant MOP-4490) (to M.S.), and Fonds Recherche France-Canada (to S.A.S. and M.S.). M.B. was supported by Ph.D. fellowships from MENRT and CANAM-Pasteur. V.J.Y. was supported by a Marie Curie fellowship (contract MEIF-2003-501887), S.B. by a Ph.D. fellowship from MENRT, and P.S. by a postdoctoral fellowship from Fondation Manlio Cantarini.

The authors of this paper declare that they have no competing financial interests.

REFERENCES

1. **Alirol, E., D. James, D. Huber, A. Marchetto, L. Vergani, J. C. Martinou, and L. Scorrano.** 2006. The mitochondrial fission protein hFis1 requires the endoplasmic reticulum gateway to induce apoptosis. Mol. Biol Cell. **17:**4593–4605.
2. **Anesti, V., and L. Scorrano.** 2006. The relationship between mitochondrial shape and function and the cytoskeleton. Biochim. Biophys. Acta **1757:**692–699.
3. **Arnoult, D., N. Rismanchi, A. Grodet, R. G. Roberts, D. P. Seeburg, J. Estaquier, M. Sheng, and C. Blackstone.** 2005. Bax/Bak-dependent release of DDP/TIMM8a promotes Drp1-mediated mitochondrial fission and mitoptosis during programmed cell death. Curr. Biol. **15:**2112–2118.
4. **Barsoum, M. J., H. Yuan, A. A. Gerencser, G. Liot, Y. Kushnareva, S. Graber, I. Kovacs, W. D. Lee, J. Waggoner, J. Cui, A. D. White, B. Bossy, J. C. Martinou, R. J. Youle, S. A. Lipton, M. H. Ellisman, G. A. Perkins, and E. Bossy-Wetzel.** 2006. Nitric oxide-induced mitochondrial fission is regulated by dynamin-related GTPases in neurons. EMBO J. **25:**3900–3911.
5. **Bellosillo, B., N. Villamor, A. Lopez-Guillermo, S. Marce, F. Bosch, E. Campo, E. Montserrat, and D. Colomer.** 2002. Spontaneous and drug-induced apoptosis is mediated by conformational changes of Bax and Bak in B-cell chronic lymphocytic leukemia. Blood **100:**1810–1816.
6. **Binet, J. L., A. Auquier, G. Dighiero, C. Chastang, H. Piguet, J. Goasguen, G. Vaugier, G. Potron, P. Colona, F. Oberling, M. Thomas, G. Tchernia, C. Jacquillat, P. Boivin, C. Lesty, M. T. Duault, M. Monconduit, S. Belabbes, and F. Gremy.** 1981. A new prognostic classification of chronic lymphocytic leukemia derived from a multivariate survival analysis. Cancer **48:**198–206.
7. **Bossy-Wetzel, E., M. J. Barsoum, A. Godzik, R. Schwarzenbacher, and S. A. Lipton.** 2003. Mitochondrial fission in apoptosis, neurodegeneration and aging. Curr. Opin. Cell Biol. **15:**706–716.
8. **Breckenridge, D. G., M. Stojanovic, R. C. Marcellus, and G. C. Shore.** 2003. Caspase cleavage product of BAP31 induces mitochondrial fission through endoplasmic reticulum calcium signals, enhancing cytochrome c release to the cytosol. J. Cell Biol. **160:**1115–1127.
9. **Brown, E. J., and W. A. Frazier.** 2001. Integrin-associated protein (CD47) and its ligands. Trends Cell Biol. **11:**130–135.
10. **Chen, H., and D. C. Chan.** 2005. Emerging functions of mammalian mitochondrial fusion and fission. Hum. Mol. Genet. **14**(Suppl. 2)**:**R283–R289.
11. **Cheson, B. D., J. M. Bennett, M. Grever, N. Kay, M. J. Keating, S. O'Brien, and K. R. Rai.** 1996. National Cancer Institute-sponsored working group guidelines for chronic lymphocytic leukemia: revised guidelines for diagnosis and treatment. Blood **87:**4990–4997.
12. **Cipolat, S., O. Martins de Brito, B. Dal Zilio, and L. Scorrano.** 2004. OPA1 requires mitofusin 1 to promote mitochondrial fusion. Proc. Natl. Acad. Sci. USA **101:**15927–15932.
13. **Cipolat, S., T. Rudka, D. Hartmann, V. Costa, L. Serneels, K. Craessaerts, K. Metzger, C. Frezza, W. Annaert, L. D'Adamio, C. Derks, T. Dejaegere, L. Pellegrini, R. D'Hooge, L. Scorrano, and B. De Strooper.** 2006. Mitochondrial rhomboid PARL regulates cytochrome c release during apoptosis via OPA1-dependent cristae remodeling. Cell **126:**163–175.
14. **Clarke, P. G.** 1990. Developmental cell death: morphological diversity and multiple mechanisms. Anat. Embryol. (Berlin) **181:**195–213.
15. **Crawford, S. E., V. Stellmach, J. E. Murphy-Ullrich, S. M. Ribeiro, J. Lawler, R. O. Hynes, G. P. Boivin, and N. Bouck.** 1998. Thrombospondin-1 is a major activator of TGF-beta1 in vivo. Cell **93:**1159–1170.
16. **Crespo, M., F. Bosch, N. Villamor, B. Bellosillo, D. Colomer, M. Rozman, S. Marce, A. Lopez-Guillermo, E. Campo, and E. Montserrat.** 2003. ZAP-70 expression as a surrogate for immunoglobulin-variable-region mutations in chronic lymphocytic leukemia. N. Engl. J. Med. **348:**1764–1775.
17. **Daiber, A., M. Oelze, M. August, M. Wendt, K. Sydow, H. Wieboldt, A. L. Kleschyov, and T. Munzel.** 2004. Detection of superoxide and peroxynitrite in model systems and mitochondria by the luminol analogue L-012. Free Radic. Res. **38:**259–269.
18. **Danial, N. N., and S. J. Korsmeyer.** 2004. Cell death: critical control points. Cell **116:**205–219.
19. **Doerfler, P., K. A. Forbush, and R. M. Perlmutter.** 2000. Caspase enzyme activity is not essential for apoptosis during thymocyte development. J. Immunol. **164:**4071–4079.
20. **Doyen, V., M. Rubio, D. Braun, T. Nakajima, J. Abe, H. Saito, G. Delespesse, and M. Sarfati.** 2003. Thrombospondin 1 is an autocrine negative regulator of human dendritic cell activation. J. Exp. Med. **198:**1277–1283.
21. **Duan, S., P. Hajek, C. Lin, S. K. Shin, G. Attardi, and A. Chomyn.** 2003. Mitochondrial outer membrane permeability change and hypersensitivity to digitonin early in staurosporine-induced apoptosis. J. Biol. Chem. **278:**1346–1353.
22. **Egger, L., D. T. Madden, C. Rheme, R. V. Rao, and D. E. Bredesen.** 2007. Endoplasmic reticulum stress-induced cell death mediated by the proteasome. Cell Death Differ. **14:**1172–1180.
23. **Fearnhead, H. O., A. J. Rivett, D. Dinsdale, and G. M. Cohen.** 1995. A pre-existing protease is a common effector of thymocyte apoptosis mediated by diverse stimuli. FEBS Lett. **357:**242–246.
24. **Finucane, D. M., E. Bossy-Wetzel, N. J. Waterhouse, T. G. Cotter, and D. R. Green.** 1999. Bax-induced caspase activation and apoptosis via cytochrome c release from mitochondria is inhibitable by Bcl-xL. J. Biol. Chem. **274:**2225–2233.
25. **Frank, S., B. Gaume, E. S. Bergmann-Leitner, W. W. Leitner, E. G. Robert, F. Catez, C. L. Smith, and R. J. Youle.** 2001. The role of dynamin-related

protein 1, a mediator of mitochondrial fission, in apoptosis. Dev. Cell. **1:**515–525.

26. **Frezza, C., S. Cipolat, O. Martins de Brito, M. Micaroni, G. V. Beznoussenko, T. Rudka, D. Bartoli, R. S. Polishuck, N. N. Danial, B. De Strooper, and L. Scorrano.** 2006. OPA1 controls apoptotic cristae remodeling independently from mitochondrial fusion. Cell **126:**177–189.
27. **Germain, M., J. P. Mathai, H. M. McBride, and G. C. Shore.** 2005. Endoplasmic reticulum BIK initiates DRP1-regulated remodelling of mitochondrial cristae during apoptosis. EMBO J. **24:**1546–1556.
28. **Gozuacik, D., and A. Kimchi.** 2004. Autophagy as a cell death and tumor suppressor mechanism. Oncogene **23:**2891–2906.
29. **Guicciardi, M. E., M. Leist, and G. J. Gores.** 2004. Lysosomes in cell death. Oncogene **23:**2881–2890.
30. **Hagnerud, S., P. P. Manna, M. Cella, A. Stenberg, W. A. Frazier, M. Colonna, and P. A. Oldenborg.** 2006. Deficit of CD47 results in a defect of marginal zone dendritic cells, blunted immune response to particulate antigen and impairment of skin dendritic cell migration. J. Immunol. **176:**5772–5778.
31. **Halestrap, A. P.** 1989. The regulation of the matrix volume of mammalian mitochondria in vivo and in vitro and its role in the control of mitochondrial metabolism. Biochim. Biophys. Acta **973:**355–382.
32. **He, H., M. Lam, T. S. McCormick, and C. W. Distelhorst.** 1997. Maintenance of calcium homeostasis in the endoplasmic reticulum by Bcl-2. J. Cell Biol. **138:**1219–1228.
33. **Imoto, M., I. Tachibana, and R. Urrutia.** 1998. Identification and functional characterization of a novel human protein highly related to the yeast dynamin-like GTPase Vps1p. J. Cell Sci. **111:**1341–1349.
34. **Ishihara, N., Y. Fujita, T. Oka, and K. Mihara.** 2006. Regulation of mitochondrial morphology through proteolytic cleavage of OPA1. EMBO J. **25:**2966–2977.
35. **Jaattela, M., and J. Tschopp.** 2003. Caspase-independent cell death in T lymphocytes. Nat. Immunol. **4:**416–423.
36. **James, D. I., P. A. Parone, Y. Mattenberger, and J. C. Martinou.** 2003. hFis1, a novel component of the mammalian mitochondrial fission machinery. J. Biol. Chem. **278:**36373–36379.
37. **Jung, C., C. M. Higgins, and Z. Xu.** 2000. Measuring the quantity and activity of mitochondrial electron transport chain complexes in tissues of central nervous system using blue native polyacrylamide gel electrophoresis. Anal. Biochem. **286:**214–223.
38. **Kamimoto, T., Y. Nagai, H. Onogi, Y. Muro, T. Wakabayashi, and M. Hagiwara.** 1998. Dymple, a novel dynamin-like high molecular weight GTPase lacking a proline-rich carboxyl-terminal domain in mammalian cells. J. Biol. Chem. **273:**1044–1051.
39. **Karbowski, M., Y. J. Lee, B. Gaume, S. Y. Jeong, S. Frank, A. Nechushtan, A. Santel, M. Fuller, C. L. Smith, and R. J. Youle.** 2002. Spatial and temporal association of Bax with mitochondrial fission sites, Drp1, and Mfn2 during apoptosis. J. Cell Biol. **159:**931–938.
40. **Karbowski, M., and R. J. Youle.** 2003. Dynamics of mitochondrial morphology in healthy cells and during apoptosis. Cell Death Differ. **10:**870–880.
41. **Koch, A., M. Thiemann, M. Grabenbauer, Y. Yoon, M. A. McNiven, and M. Schrader.** 2003. Dynamin-like protein 1 is involved in peroxisomal fission. J. Biol. Chem. **278:**8597–8605.
42. **Kolb, J. P., C. Kern, C. Quiney, V. Roman, and C. Billard.** 2003. Re-establishment of a normal apoptotic process as a therapeutic approach in B-CLL. Curr. Drug Targets Cardiovasc. Haematol. Disord. **3:**261–286.
43. **Lamy, L., A. Foussat, E. J. Brown, P. Bornstein, M. Ticchioni, and A. Bernard.** 2007. Interactions between CD47 and thrombospondin reduce inflammation. J. Immunol. **178:**5930–5939.
44. **Lamy, L., M. Ticchioni, A. K. Rouquette-Jazdanian, M. Samson, M. Deckert, A. H. Greenberg, and A. Bernard.** 2003. CD47 and the 19 kDa interacting protein-3 (BNIP3) in T cell apoptosis. J. Biol. Chem. **278:**23915–23921.
45. **Latour, S., H. Tanaka, C. Demeure, V. Mateo, M. Rubio, E. J. Brown, C. Maliszewski, F. P. Lindberg, A. Oldenborg, A. Ullrich, G. Delespesse, and M. Sarfati.** 2001. Bidirectional negative regulation of human T and dendritic cells by CD47 and its cognate receptor signal-regulator protein-alpha: down-regulation of IL-12 responsiveness and inhibition of dendritic cell activation. J. Immunol. **167:**2547–2554.
46. **Lee, Y. J., S. Y. Jeong, M. Karbowski, C. L. Smith, and R. J. Youle.** 2004. Roles of the mammalian mitochondrial fission and fusion mediators fis1, drp1, and opa1 in apoptosis. Mol. Biol. Cell **15:**5001–5011.
47. **Lindberg, F. P., D. C. Bullard, T. E. Caver, H. D. Gresham, A. L. Beaudet, and E. J. Brown.** 1996. Decreased resistance to bacterial infection and granulocyte defects in IAP-deficient mice. Science **274:**795–798.
48. **Lorenzo, H. K., and S. A. Susin.** 2004. Mitochondrial effectors in caspase-independent cell death. FEBS Lett. **557:**14–20.
49. **Mainou-Fowler, T., H. M. Dignum, S. J. Proctor, and G. P. Summerfield.** 2004. The prognostic value of CD38 expression and its quantification in B cell chronic lymphocytic leukemia (B-CLL). Leuk. Lymphoma **45:**455–462.
50. **Manna, P. P., and W. A. Frazier.** 2003. The mechanism of CD47-dependent killing of T cells: heterotrimeric Gi-dependent inhibition of protein kinase A. J. Immunol. **170:**3544–3553.
51. **Martinou, J. C., and D. R. Green.** 2001. Breaking the mitochondrial barrier. Nat. Rev. Mol. Cell. Biol. **2:**63–67.
52. **Martinvalet, D., P. Zhu, and J. Lieberman.** 2005. Granzyme A induces caspase-independent mitochondrial damage, a required first step for apoptosis. Immunity **22:**355–370.
53. **Mateo, V., E. J. Brown, G. Biron, M. Rubio, A. Fischer, F. L. Deist, and M. Sarfati.** 2002. Mechanisms of CD47-induced caspase-independent cell death in normal and leukemic cells: link between phosphatidylserine exposure and cytoskeleton organization. Blood **100:**2882–2890.
54. **Mateo, V., L. Lagneaux, D. Bron, G. Biron, M. Armant, G. Delespesse, and M. Sarfati.** 1999. CD47 ligation induces caspase-independent cell death in chronic lymphocytic leukemia. Nat. Med. **5:**1277–1284.
55. **Olichon, A., L. Baricault, N. Gas, E. Guillou, A. Valette, P. Belenguer, and G. Lenaers.** 2003. Loss of OPA1 perturbates the mitochondrial inner membrane structure and integrity, leading to cytochrome c release and apoptosis. J. Biol. Chem. **278:**7743–7746.
56. **Pardo, J., P. Perez-Galan, S. Gamen, I. Marzo, I. Monleon, A. A. Kaspar, S. A. Susin, G. Kroemer, A. M. Krensky, J. Naval, and A. Anel.** 2001. A role of the mitochondrial apoptosis-inducing factor in granulysin-induced apoptosis. J. Immunol. **167:**1222–1229.
57. **Parone, P. A., D. I. James, S. Da Cruz, Y. Mattenberger, O. Donze, F. Barja, and J. C. Martinou.** 2006. Inhibiting the mitochondrial fission machinery does not prevent Bax/Bak-dependent apoptosis. Mol. Cell. Biol. **26:**7397–7408.
58. **Pettersen, R. D., K. Hestdal, M. K. Olafsen, S. O. Lie, and F. P. Lindberg.** 1999. CD47 signals T cell death. J. Immunol. **162:**7031–7040.
59. **Pitts, K. R., M. A. McNiven, and Y. Yoon.** 2004. Mitochondria-specific function of the dynamin family of protein DLP1 is mediated by its C-terminal domains. J. Biol. Chem. **279:**50286–50294.
60. **Pitts, K. R., Y. Yoon, E. W. Krueger, and M. A. McNiven.** 1999. The dynamin-like protein DLP1 is essential for normal distribution and morphology of the endoplasmic reticulum and mitochondria in mammalian cells. Mol. Biol. Cell **10:**4403–4417.
61. **Pritsch, O., X. Troussard, C. Magnac, F. R. Mauro, F. Davi, B. Payelle-Brogard, G. Dumas, M. Pulik, F. Clerget, F. Mandelli, N. Chiorazzi, H. W. Schroeder, Jr., M. Leporrier, and G. Dighiero.** 1999. VH gene usage by family members affected with chronic lymphocytic leukaemia. Br. J. Haematol. **107:**616–624.
62. **Rebres, R. A., J. M. Green, M. I. Reinhold, M. Ticchioni, and E. J. Brown.** 2001. Membrane raft association of CD47 is necessary for actin polymerization and protein kinase C theta translocation in its synergistic activation of T cells. J. Biol. Chem. **276:**7672–7680.
63. **Ricci, J. E., R. A. Gottlieb, and D. R. Green.** 2003. Caspase-mediated loss of mitochondrial function and generation of reactive oxygen species during apoptosis. J. Cell Biol. **160:**65–75.
64. **Ricci, J. E., C. Munoz-Pinedo, P. Fitzgerald, B. Bailly-Maitre, G. A. Perkins, N. Yadava, I. E. Scheffler, M. H. Ellisman, and D. R. Green.** 2004. Disruption of mitochondrial function during apoptosis is mediated by caspase cleavage of the p75 subunit of complex I of the electron transport chain. Cell **117:**773–786.
65. **Roue, G., N. Bitton, V. J. Yuste, T. Montange, M. Rubio, F. Dessauge, C. Delettre, H. Merle-Beral, M. Sarfati, and S. A. Susin.** 2003. Mitochondrial dysfunction in CD47-mediated caspase-independent cell death: ROS production in the absence of cytochrome c and AIF release. Biochimie **85:**741–746.
66. **Rube, D. A., and A. M. van der Bliek.** 2004. Mitochondrial morphology is dynamic and varied. Mol. Cell. Biochem. **257:**331–339.
67. **Santel, A., S. Frank, B. Gaume, M. Herrler, R. J. Youle, and M. T. Fuller.** 2003. Mitofusin-1 protein is a generally expressed mediator of mitochondrial fusion in mammalian cells. J. Cell Sci. **116:**2763–2774.
68. **Sarfati, M., S. Chevret, C. Chastang, G. Biron, P. Stryckmans, G. Delespesse, J. L. Binet, H. Merle-Beral, and D. Bron.** 1996. Prognostic importance of serum soluble CD23 level in chronic lymphocytic leukemia. Blood **88:**4259–4264.
69. **Saumet, A., M. B. Slimane, M. Lanotte, J. Lawler, and V. Dubernard.** 2005. Type 3 repeat/C-terminal domain of thrombospondin-1 triggers caspase-independent cell death through CD47/alphavbeta3 in promyelocytic leukemia NB4 cells. Blood **106:**658–667.
70. **Savill, J., I. Dransfield, C. Gregory, and C. Haslett.** 2002. A blast from the past: clearance of apoptotic cells regulates immune responses. Nat. Rev. Immunol. **2:**965–975.
71. **Sayers, T. J., A. D. Brooks, N. Seki, M. J. Smyth, H. Yagita, B. R. Blazar, and A. M. Malyguine.** 2000. T cell lysis of murine renal cancer: multiple signaling pathways for cell death via Fas. J. Leukoc. Biol. **68:**81–86.
72. **Schagger, H.** 1995. Quantification of oxidative phosphorylation enzymes after blue native electrophoresis and two-dimensional resolution: normal complex I protein amounts in Parkinson's disease conflict with reduced catalytic activities. Electrophoresis **16:**763–770.
73. **Schweichel, J. U., and H. J. Merker.** 1973. The morphology of various types of cell death in prenatal tissues. Teratology **7:**253–266.
74. **Shin, H. W., C. Shinotsuka, S. Torii, K. Murakami, and K. Nakayama.** 1997. Identification and subcellular localization of a novel mammalian dynamin-

related protein homologous to yeast Vps1p and Dnm1p. J. Biochem. (Tokyo) **122:**525–530.
75. **Smirnova, E., D. L. Shurland, S. N. Ryazantsev, and A. M. van der Bliek.** 1998. A human dynamin-related protein controls the distribution of mitochondria. J. Cell Biol. **143:**351–358.
76. **Stojanovski, D., O. S. Koutsopoulos, K. Okamoto, and M. T. Ryan.** 2004. Levels of human Fis1 at the mitochondrial outer membrane regulate mitochondrial morphology. J. Cell Sci. **117:**1201–1210.
77. **Sugioka, R., S. Shimizu, and Y. Tsujimoto.** 2004. Fzo1, a protein involved in mitochondrial fusion, inhibits apoptosis. J. Biol. Chem. **279:**52726–52734.
78. **Susin, S. A., H. K. Lorenzo, N. Zamzami, I. Marzo, B. E. Snow, G. M. Brothers, J. Mangion, E. Jacotot, P. Costantini, M. Loeffler, N. Larochette, D. R. Goodlett, R. Aebersold, D. P. Siderovski, J. M. Penninger, and G. Kroemer.** 1999. Molecular characterization of mitochondrial apoptosis-inducing factor. Nature **397:**441–446.
79. **Susin, S. A., N. Zamzami, M. Castedo, T. Hirsch, P. Marchetti, A. Macho, E. Daugas, M. Geuskens, and G. Kroemer.** 1996. Bcl-2 inhibits the mitochondrial release of an apoptogenic protease. J Exp. Med. **184:**1331–1341.
80. **Tada, K., M. Tanaka, R. Hanayama, K. Miwa, A. Shinohara, A. Iwamatsu, and S. Nagata.** 2003. Tethering of apoptotic cells to phagocytes through binding of CD47 to Src homology 2 domain-bearing protein tyrosine phosphatase substrate-1. J. Immunol. **171:**5718–5726.
81. **Tsujimoto, Y.** 2002. Bcl-2 family of proteins: life-or-death switch in mitochondria. Biosci. Rep. **22:**47–58.
82. **Uzzo, R. G., N. Dulin, T. Bloom, R. Bukowski, J. H. Finke, and V. Kolenko.** 2001. Inhibition of NFkappaB induces caspase-independent cell death in human T lymphocytes. Biochem. Biophys. Res. Commun. **287:**895–899.
83. **Van, V. Q., S. Lesage, S. Bouguermouh, P. Gautier, M. Rubio, M. Levesque, S. Nguyen, L. Galibert, and M. Sarfati.** 2006. Expression of the self-marker CD47 on dendritic cells governs their trafficking to secondary lymphoid organs. EMBO J. **25:**5560–5568.
84. **Varadi, A., L. I. Johnson-Cadwell, V. Cirulli, Y. Yoon, V. J. Allan, and G. A. Rutter.** 2004. Cytoplasmic dynein regulates the subcellular distribution of mitochondria by controlling the recruitment of the fission factor dynamin-related protein-1. J. Cell Sci. **117:**4389–4400.
85. **Yoon, Y., E. W. Krueger, B. J. Oswald, and M. A. McNiven.** 2003. The mitochondrial protein hFis1 regulates mitochondrial fission in mammalian cells through an interaction with the dynamin-like protein DLP1. Mol. Cell. Biol. **23:**5409–5420.
86. **Yoon, Y., K. R. Pitts, S. Dahan, and M. A. McNiven.** 1998. A novel dynamin-like protein associates with cytoplasmic vesicles and tubules of the endoplasmic reticulum in mammalian cells. J. Cell Biol. **140:**779–793.
87. **Yu, T., R. J. Fox, L. S. Burwell, and Y. Yoon.** 2005. Regulation of mitochondrial fission and apoptosis by the mitochondrial outer membrane protein hFis1. J. Cell Sci. **118:**4141–4151.
88. **Zamzami, N., S. A. Susin, P. Marchetti, T. Hirsch, I. Gomez-Monterrey, M. Castedo, and G. Kroemer.** 1996. Mitochondrial control of nuclear apoptosis. J Exp. Med. **183:**1533–1544.
89. **Zhu, P. P., A. Patterson, J. Stadler, D. P. Seeburg, M. Sheng, and C. Blackstone.** 2004. Intra- and intermolecular domain interactions of the C-terminal GTPase effector domain of the multimeric dynamin-like GTPase Drp1. J. Biol. Chem. **279:**35967–35974.
90. **Zornig, M., A. Hueber, W. Baum, and G. Evan.** 2001. Apoptosis regulators and their role in tumorigenesis. Biochim. Biophys. Acta **1551:**F1–F37.